Elimination from Wastewater of Antibiotics Reserved for Hospital Settings, with a Fenton Process Based on Zero-Valent Iron

SUPPLEMENTARY MATERIAL

Elimination from Wastewater of Antibiotics Reserved for Hospital Settings, with a Fenton Process Based on Zero-Valent Iron (ZVI-Fenton)

Francesco Furia,[a] Marco Minella,[a] Fabio Gosetti,[b] Raffaella Sabatino,[c] Andrea Di Cesare,[c] Gianluca Corno,[c] Davide Vione [a]*

[a] *Dipartimento di Chimica, Università di Torino, Via Pietro Giuria 5, 10125 Torino, Italy.*

[b] *Dipartimento di Scienze dell'Ambiente e della Terra, Università di Milano – Bicocca, Piazza della Scienza 1, 20126 Milano, Italy.*

[c] *Molecular Ecology Group, National Research Council of Italy, Water Research Institute, Largo Tonolli 50, 28922, Verbania (VCO), Italy.*

* Corresponding author. E-mail: *davide.vione@unito.it*

Table of contents

S1. Reagents

Cefazolin (CFZ, EP reference standard), imipenem (IMI, reference standard), vancomycin (VNM, pharmaceutical secondary standard), $HClO_4$ (70% w/w), NaOH (≥90%), methanol (gradient grade), H_2SO_4 (96% w/w), H_3PO_4 (85% w/w), $FeCl_3 \cdot 6\ H_2O$ (99%), ampyrone (4-amino-2,3-dimethyl-1-phenyl-3-pyrazol-5-one; reagent grade), NaH_2PO_4 (≥99.9%), Na_2HPO_4 (≥98%), ZVI (≥99.5%, powder < 10 μm, product number 44890), 1,10-phenanthroline (>99%), ascorbic acid (reagent grade), 5,5-dimethyl-1-pyrrolidine-N-oxide (DMPO, 97%), catalase and horseradish peroxidase were purchased from Sigma-Aldrich; KSCN (≥98%) and $FeSO_4 \cdot 7\ H_2O$ (99.5%) from Merck; H_2O_2 (30% w/v) from Applichem PanReac; formalin, SYBRgreen and propidium iodide from Thermo-Fisher Scientific. These reagents were used as received, without further purification, with the exception of DMPO that was stored at –15°C, diluted to 0.15 mol L^{-1} in ultra-pure water before use, and filtered on activated carbon to eliminate impurities and degradation products. The water used was of Milli-Q quality.

S2. Wastewater characterization

The wastewater samples WWa and WWb were characterized for conductivity (HI2030 Multi-parameter probe, Hanna Instruments), pH (Checker HI98103, Hanna Instruments), total carbon (TC), inorganic carbon (IC), total organic carbon (computed as TOC = TC – IC) and total nitrogen (TN, Shimadzu ON-LINE TOC-VCSH instrument, equipped with an ASI-V autosampler and fed with zero-grade air), as well as the anions Cl^-, NO_3^- and SO_4^{2-} (Dionex DX 500 ion chromatograph, Dionex Ion Pac AS9-HC column, elution with 9 mM K_2CO_3 at 1 mL min^{-1}). The results are reported in **Table S1** below.

Table S1. Physico-chemical features of the studied wastewater samples. TC = total carbon, TOC = total organic carbon, IC = inorganic carbon, TN = total nitrogen. The error bounds represent the standard error of replicate measurements.

Parameter	WWa	WWb
Conductivity, µS cm^{-1}	267±9	914±22
pH	7.5±0.1	7.8±0.1
TC, mg_C L^{-1}	10.5±0.4	44.6±0.8
TOC, mg_C L^{-1}	7.8±0.6	38.9±1.1
IC, mg_C L^{-1}	2.7±0.2	5.7±0.3
TN, mg_N L^{-1}	5.8±0.7	6.5±0.6
Chloride (Cl^-), mg L^{-1}	35.6±2.2	109.5±5.4
Nitrate (NO_3^-), mg L^{-1}	34.7±2.8	37.9±1.9
Sulfate (SO_4^{2-}), mg L^{-1}	19.6±1.2	151±2.1

S3. Instrumentation details

Liquid chromatography

It was used a VWR-Hitachi Elite LaChrom instrument equipped with L2455 diode array detector (DAD), L2130 quaternary pump module, L2300 column oven (set at 40 °C), L2200 autosampler (sample injection volume 60 µL), Duratec vacuum degasser and reverse-phase column Merck LiChroCART, packed with LiChrospher 100 RP18 (125 mm × 4 mm × 5 µm). The chromatographic elution and detection conditions are reported in **Table S2** below (flow rate was 1.0 mL min^{-1}.

Table S2. Chromatographic conditions used for the elution, separation (where relevant) and detection of the antibiotics under study.

Compound	Eluent A	Eluent B	Conditions	t_R, min	$\lambda_{detection}$, nm
CFZ+VNM +IMI	Methanol	$H_2PO_4^-/HPO_4^{2-}$, pH 7	0-1.50 min: 4% A; 2.00-9.00 min: 26% A; 9.50-15.00 min: 4% A	2.60 (IMI) 6.45 (CFZ) 9.00 (VNM)	299 (IMI) 271 (CFZ) 281 (VNM)

Colorimetric methods for Fe(II), Fe(III) and H_2O_2

At scheduled reaction times, samples were withdrawn from the reaction mixture and filtered (0.45 μm) to remove suspended ZVI. In these experiments methanol was not used as quencher to avoid analytical biases, thus the following determinations were done soon after sample withdrawal. Absorbance measurements were carried out with a Varian Cary 100 Scan double-beam UV-Vis spectrophotometer, using Hellma quartz cuvettes with 1 cm optical path length. Dissolved Fe(II) was determined by exploiting its reaction with o-phenanthroline (4×10^{-3} mol L^{-1}, pH 3 by 4×10^{-3} mol L^{-1} $H_3PO_4/H_2PO_4^-$), which yields a red-orange complex with molar absorption coefficient ε_{510nm} = 1.1×10^4 L mol^{-1} cm^{-1}. Total Fe (Fe_{TOT}) was determined on another sample aliquot, after Fe(III) reduction to Fe(II) upon addition of ascorbic acid (4×10^{-4} mol L^{-1}) for a reaction time of 20 min. Dissolved Fe(III) was then calculated as Fe(III) = Fe_{TOT} - Fe(II). Hydrogen peroxide was determined with the peroxidase - 4-aminoantipyrine method, which is based on the formation of a colored quinoneimine dye that absorbs at 505 nm.

Identification of degradation intermediates by UHPLC-MS/MS

A liquid chromatograph Nexera Shimadzu (Kyoto, Japan) was used, equipped with a DGU-20A3R Degasser, two LC-30AD Pumps, a SIL-30AC Autosampler, a CTO-20AC column compartment and a CMB-20A Lite system controller. The system was interfaced with a 3200 QTrap™ mass spectrometer (Sciex, Concord, Canada) by a Turbo V™ interface equipped with an ESI probe. The 3200 QTrap™ data were processed by Analyst 1.5.2 (Toronto, Canada) and Peakview 1.2 (Toronto, Canada) software.

The stationary phase was a Kinetex C18 column (3.0 mm × 100 mm, 1.7 μm) (Phenomenex, Bologna, Italy). The mobile phase was a mixture of water (A) and methanol (B), both with the addition of 0.1% formic acid, eluting at a flow rate of 0.400 mL min^{-1}. The final gradient conditions of UHPLC-MS/MS, working in selected reaction monitoring (SRM) mode, were the following: 0.0-

1.0 min 5% B, 1.0-15.0 min 50% B, 15.0-15.1 min 98% B, 15.1-17.0 min 98% B, 17.0-17.1 min 5% B, the latter kept till 20.0 min . The injection volume was 10.0 µL and the oven temperature was set at 40 °C.

The turbo ion spray ionization (TIS) was obtained using the Turbo V^{TM} interface working in positive ion (PI) mode. The instrumental parameters were set as follows: curtain gas (N_2) at 40 psig, nebulizer gas GS1 (N_2) and GS2 (N_2) at 75 and 70 psig, respectively, desolvation temperature (TEM) at 500 °C, collision activated dissociation gas (CAD) at 6 units (arbitrary scale), and ion spray voltage (IS) at +5000 V. The declustering potential (DP) and the entrance potential (EP) were set at +40 V and +4 V, respectively, in both the MS and MS/MS experiments. The collision energy (CE) was set at +10 in MS experiment, and at +45 V with the addition of ±15 V due to the collision energy spread (CES) in the Enhanced Product Ion (EPI) experiments. Unit mass resolution was established and maintained in each mass-resolving quadrupole, by keeping a full width at half maximum (FWHM) of about 0.7 u.

In order to identify the unknown degradation products of the antibiotics investigated, the hybrid quadrupole-ion trap (QLIT) mass analyzer was used in dual mode. First, the analyzer worked in data-dependent mode using the third quadrupole as linear ion trap, in order to identify the characteristic *m/z* signals of the corresponding antibiotic precursors. Secondly, the precursor-product ion transitions were chosen to build a more sensitive SRM method using the analyzer as triple quadrupole. The non-target screening was carried out with Enhanced MS experiment (EMS), *i.e.*, a full scan mode as a survey scan. When the signal of a detected compound exceeded a defined threshold, the survey scan automatically triggered the acquisition of both Enhanced Resolution (ER) and Enhanced Product Ion (EPI). The MS worked cyclizing an Enhanced MS experiment (EMS) as survey scan at 1000 Da/s between *m/z* 100 and *m/z* 650, using dynamic background subtraction of survey scan.

The data-dependent acquisition conditions that had to be satisfied in order to trigger the dependent scans were as follows: the survey scan ion must be greater than *m/z* 100 and smaller than *m/z* 650,

and it must exceed the threshold of 100,000 cps. The ion could be monitored 3 times (number of occurrences) before it was excluded from future scans for 5 s. If these conditions were satisfied, then two different dependent scans were performed on the most intense ion: the Enhanced Resolution (ER) experiment as first dependent scan at 250 Da/s, and the EPI experiment as second dependent scan at 1000 Da/s (number of scans to sum = 2). The total cycle time of the analysis was 1.7 s. The SRM method was defined once the precursor/product ion transitions were assigned to each chromatographic peak.

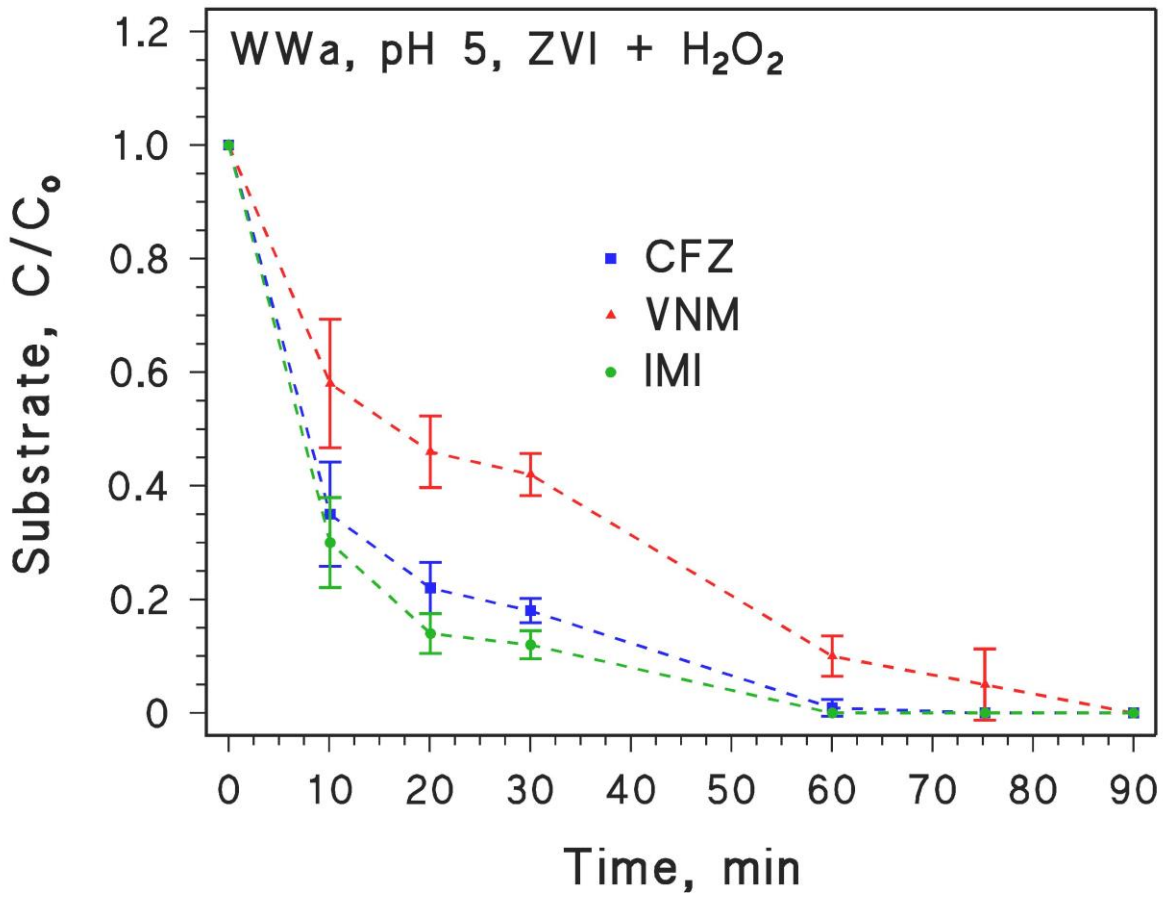

Figure S1. Repeatability test on the degradation of a mixture of 4 µmol L^{-1} cefazolin (CFZ) + 4 µmol L^{-1} vancomycin (VNM) + 4 µmol L^{-1} imipenem (IMI) in secondary wastewater (WWa) at pH 5, adjusted with H_2SO_4 before the beginning of the reaction and corrected again at 30 min. Other conditions: 0.02 g L^{-1} ZVI; 400 µmol L^{-1} H_2O_2 added in three aliquots (300 µmol L^{-1} at 0 min, 50 µmol L^{-1} at 30 min, and 50 µmol L^{-1} at 60 min). The data points plus error bars represent the average values and standard deviation of experiments carried out in triplicate.

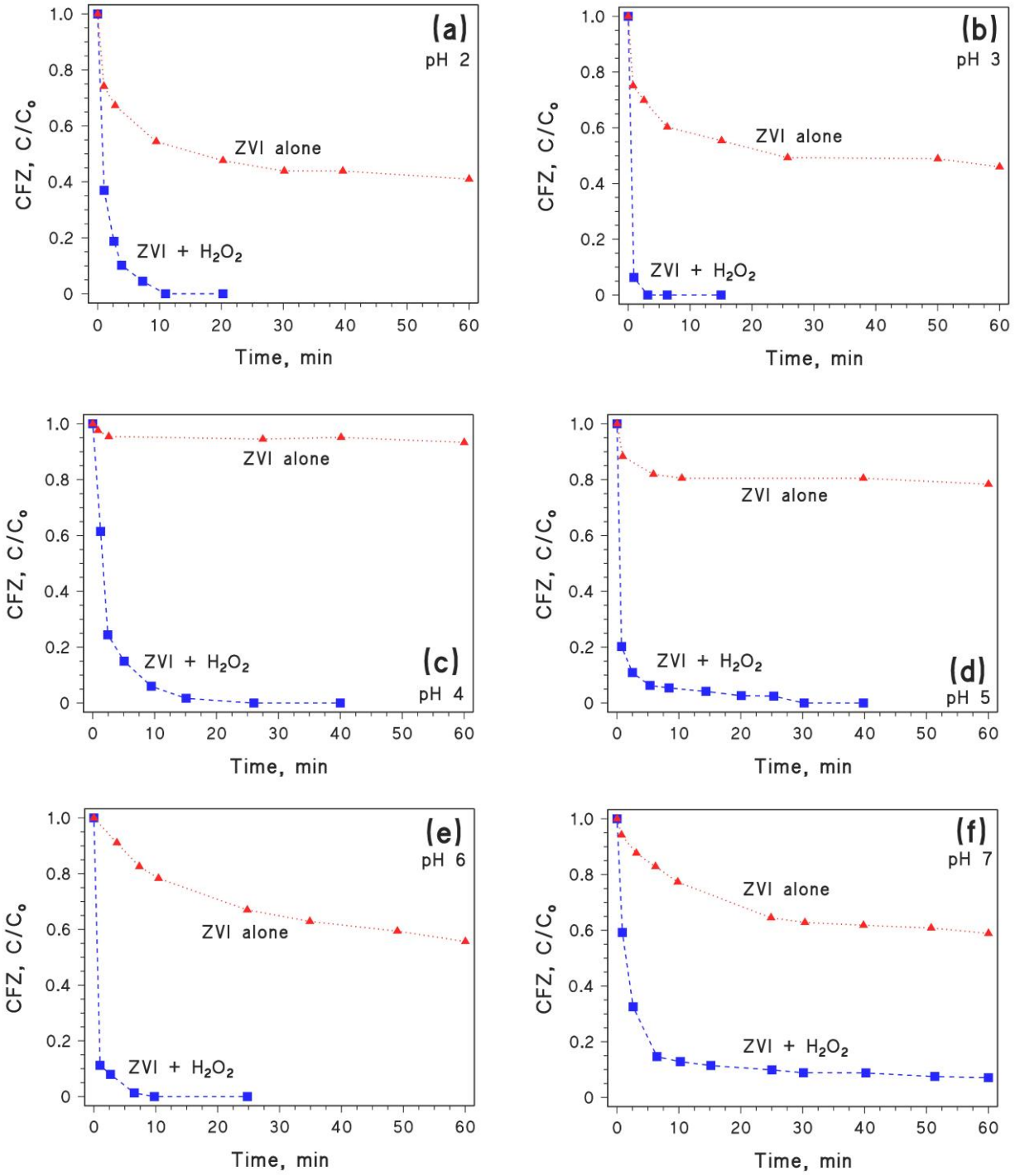

Figure S2. Degradation of 10 µmol L^{-1} cefazolin (CFZ) in the presence of ZVI + H_2O_2 and of ZVI alone. **(a)** pH 2, 50 µmol L^{-1} H_2O_2, 0.01 g L^{-1} ZVI; **(b)** pH 3, 50 µmol L^{-1} H_2O_2, 0.01 g L^{-1} ZVI; **(c)** pH 4, 50 µmol L^{-1} H_2O_2, 0.01 g L^{-1} ZVI; **(d)** pH 5, 100 µmol L^{-1} H_2O_2, 0.01 g L^{-1} ZVI; **(e)** pH 6, 400 µmol L^{-1} H_2O_2, 0.02 g L^{-1} ZVI; **(f)** pH 7, 400 µmol L^{-1} H_2O_2, 0.03 g L^{-1} ZVI.

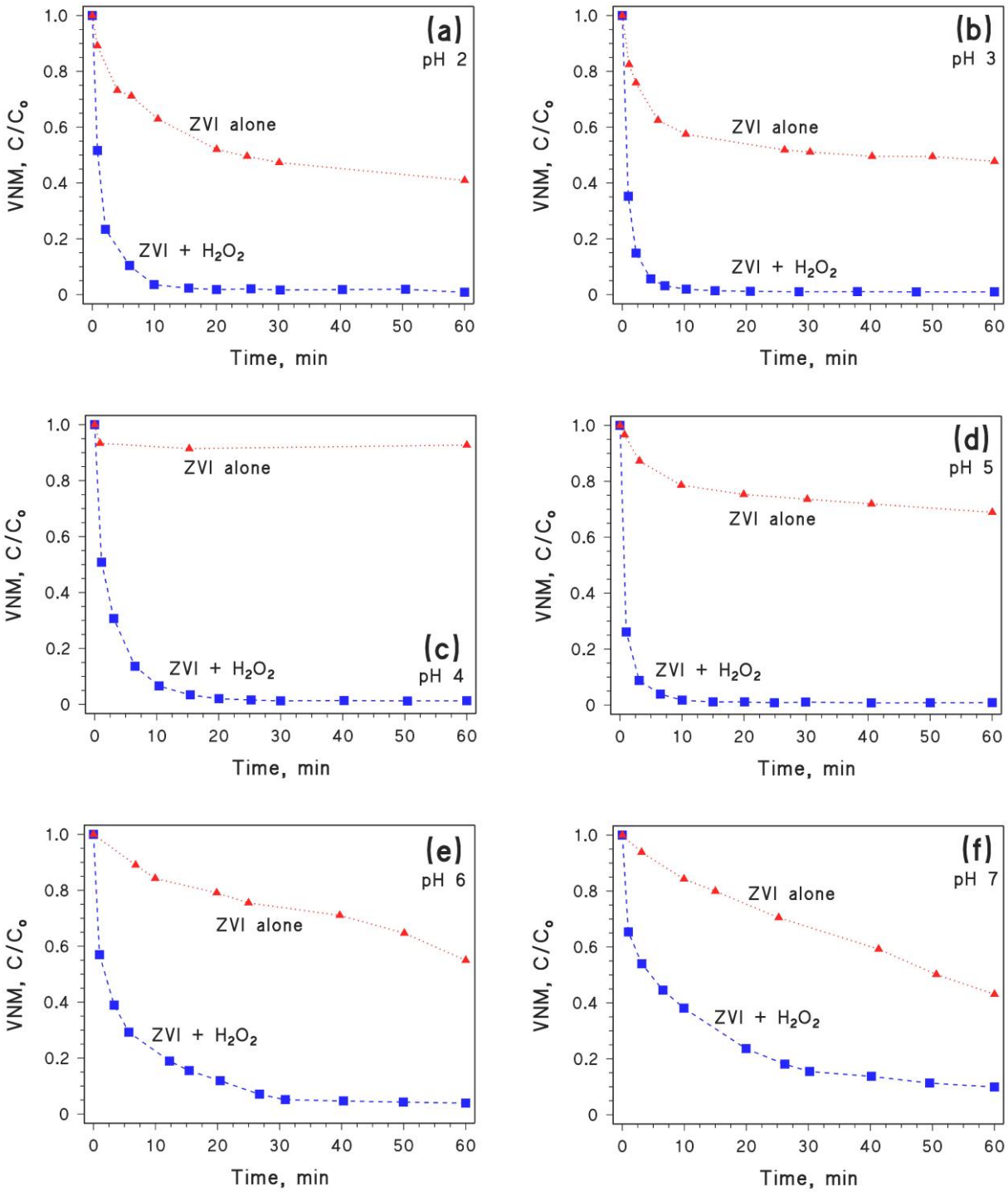

Figure S3. Degradation of 10 µmol L^{-1} vancomicin (VNM) in the presence of ZVI + H_2O_2 and of ZVI alone. **(a)** pH 2, 50 µmol L^{-1} H_2O_2, 0.01 g L^{-1} ZVI; **(b)** pH 3, 50 µmol L^{-1} H_2O_2, 0.01 g L^{-1} ZVI; **(c)** pH 4, 80 µmol L^{-1} H_2O_2, 0.01 g L^{-1} ZVI; **(d)** pH 5, 200 µmol L^{-1} H_2O_2, 0.02 g L^{-1} ZVI; **(e)** pH 6, 400 µmol L^{-1} H_2O_2, 0.03 g L^{-1} ZVI; **(f)** pH 7, 200 µmol L^{-1} H_2O_2, 0.03 g L^{-1} ZVI.

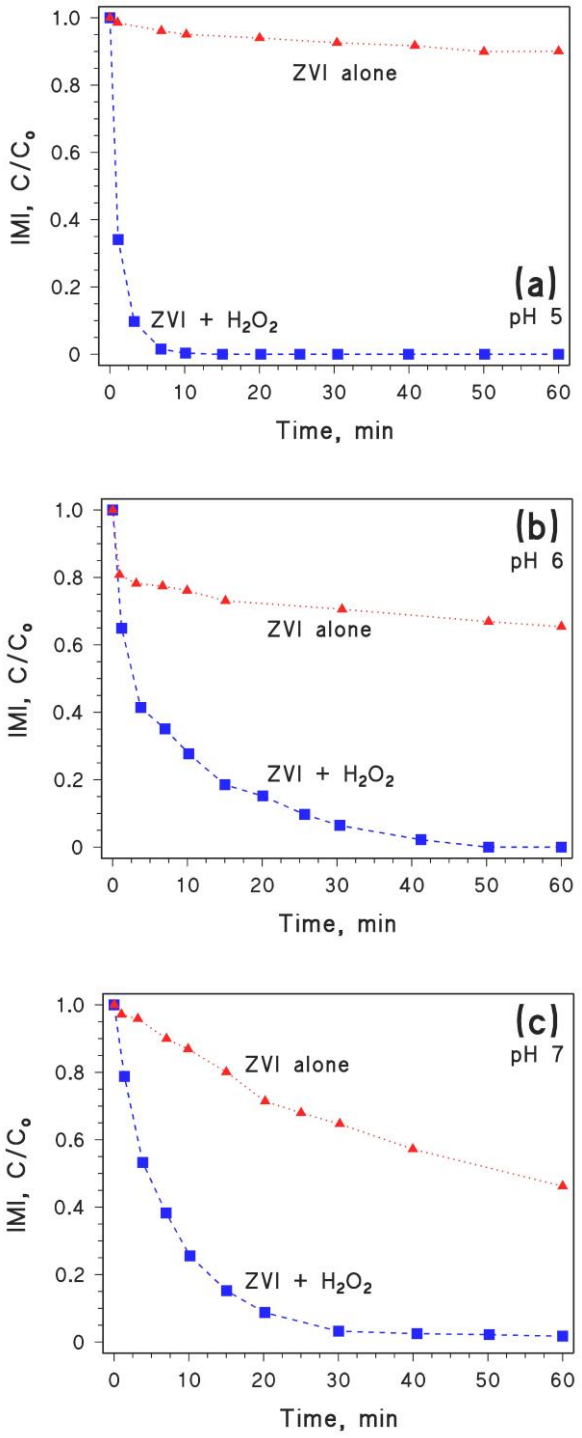

Figure S4. Degradation of 10 µmol L^{-1} imipenem (IMI) in the presence of ZVI + H_2O_2 and of ZVI alone. **(a)** pH 5, 100 µmol L^{-1} H_2O_2, 0.01 g L^{-1} ZVI; **(b)** pH 6, 200 µmol L^{-1} H_2O_2, 0.02 g L^{-1} ZVI; **(f)** pH 7, 200 µmol L^{-1} H_2O_2, 0.04 g L^{-1} ZVI.

Table S3. Summary of the preliminary ZVI - Fenton degradation experiments carried out with ultra-pure water in the pH interval 5-7. ZVI and H_2O_2 were added only once, at the beginning of the reaction.

pH	ZVI, g L^{-1}	H_2O_2, mol L^{-1}	Removal percentage after 60 min		
			CFZ	VNM	IMI
5	0.01	1.0×10^{-4}	99	92	99
5	0.01	2.0×10^{-4}	67	59	82
5	0.02	2.0×10^{-4}	89	83	96
6	0.02	2.0×10^{-4}	54	65	63
6	0.02	4.0×10^{-4}	44	45	75
6	0.03	2.0×10^{-4}	59	68	66
6	0.03	4.0×10^{-4}	49	58	62
7	0.03	2.0×10^{-4}	35	45	57
7	0.03	4.0×10^{-4}	20	21	49
7	0.04	2.0×10^{-4}	65	77	74

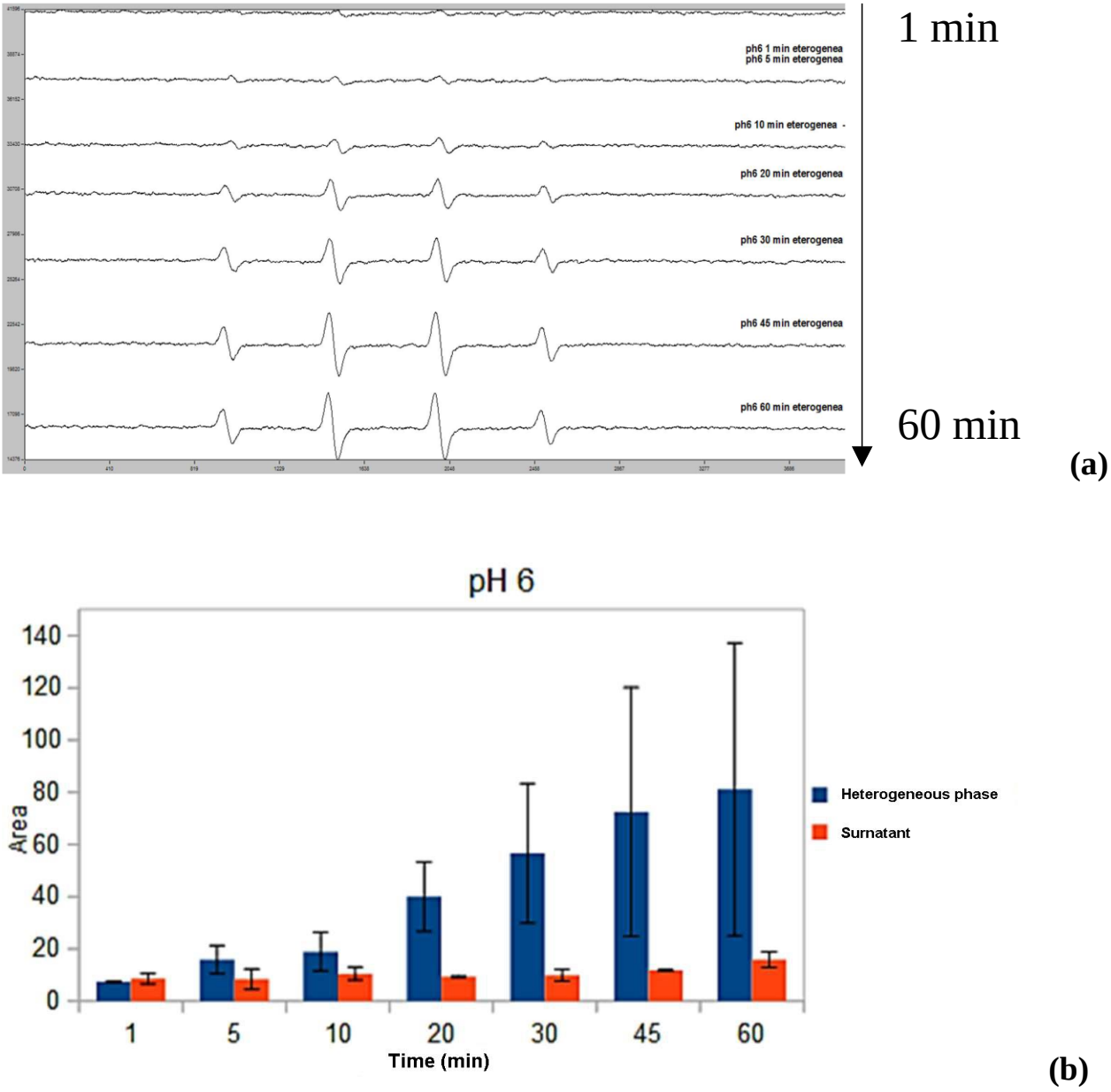

Figure S5. (a) Time evolution of the EPR spectra of a solution containing 0.06 mol L^{-1} DMPO, 0.1 g L^{-1} ZVI and 0.001 mol L^{-1} H_2O_2 at pH 6, adjusted with a phosphate buffer. The reported EPR signals are those of the DMPO-OH adduct. **(b)** Comparison between the DMPO-OH EPR signals observed in the ZVI-Fenton system and in the surnatant. In the latter case, ZVI + H_2O_2 (without DMPO) was stirred for 1 h, after which the suspension was filtered and DMPO added. Samples were withdrawn after the reported time following DMPO addition.

Table S4. Summary of the ZVI - Fenton degradation experiments carried out with WWb upon acidification with H_2SO_4 at pH 6. The highlighted conditions are those reported in **Figure S6b**. Compared to those conditions, worse results were obtained by either increasing or decreasing the H_2O_2 concentration/ZVI loading. Note that wastewater has a minimum in its buffer capacity at 4 < pH < 6, thus the amount of H_2SO_4 needed to fix pH to 6 was not much different than that needed to fix pH to 5 (see **Figure S7**).

#	Total ZVI, g L^{-1}	Total H_2O_2, mol L^{-1}	Removal percentage after 90 min		
			CFZ	VNM	IMI
1	0.02	1.0×10^{-4}	19	35	57
2	0.03	1.0×10^{-4}	0	69	0
3	0.03	2.0×10^{-4}	43	39	73
4	0.03	3.0×10^{-4}	31	32	57
5	0.04	1.0×10^{-4}	23	41	58
6	0.04	2.5×10^{-4}	23	33	70
7	**0.04**	**4.0×10^{-4}**	**63**	**55**	**88**
8	0.05	5.0×10^{-4}	25	21	37
9	0.06	2.0×10^{-4}	17	24	33
10	0.06	3.5×10^{-4}	41	38	63
11	0.08	2.0×10^{-4}	21	31	62
12	0.10	4.0×10^{-4}	28	29	28

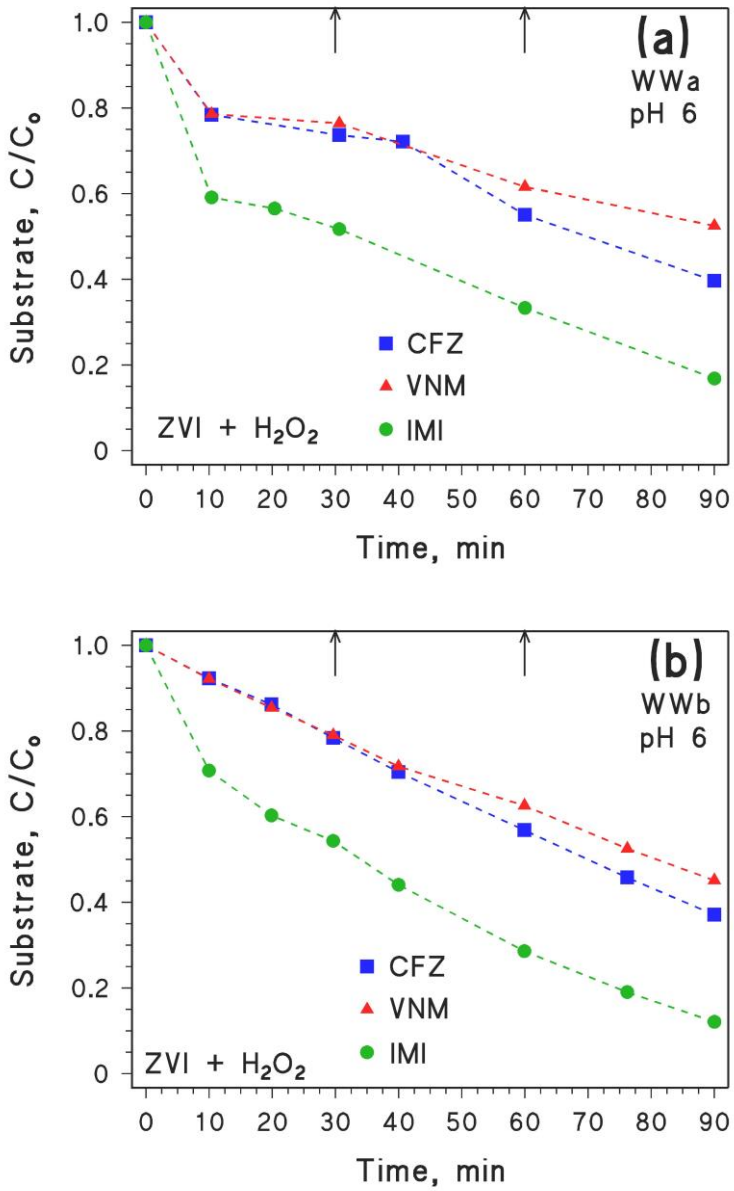

Figure S6. Degradation of a mixture of 4 µmol L^{-1} CFZ + 4 µmol L^{-1} VNM + 4 µmol L^{-1} IMI in wastewater. **(a)** WWa at pH 6, fixed by H_2SO_4 and corrected when necessary during the course of the reaction; 0.04 g L^{-1} ZVI added in two aliquots (half at 0 min and half at 30 min); 400 µmol L^{-1} H_2O_2 added in three aliquots (300 µmol L^{-1} at 0 min, 50 µmol L^{-1} at 30 min, and 50 µmol L^{-1} at 60 min). **(b)** WWb at pH 6, fixed by H_2SO_4 and corrected when necessary during the course of the reaction; 0.04 g L^{-1} ZVI added in two aliquots (half at 0 min and half at 30 min); 400 µmol L^{-1} H_2O_2 added in three aliquots (300 µmol L^{-1} at 0 min, 50 µmol L^{-1} at 30 min, and 50 µmol L^{-1} at 60 min).

The time points at 30 and 60 min (further additions of H_2O_2 and, where applicable, ZVI) are highlighted by the vertical arrows.

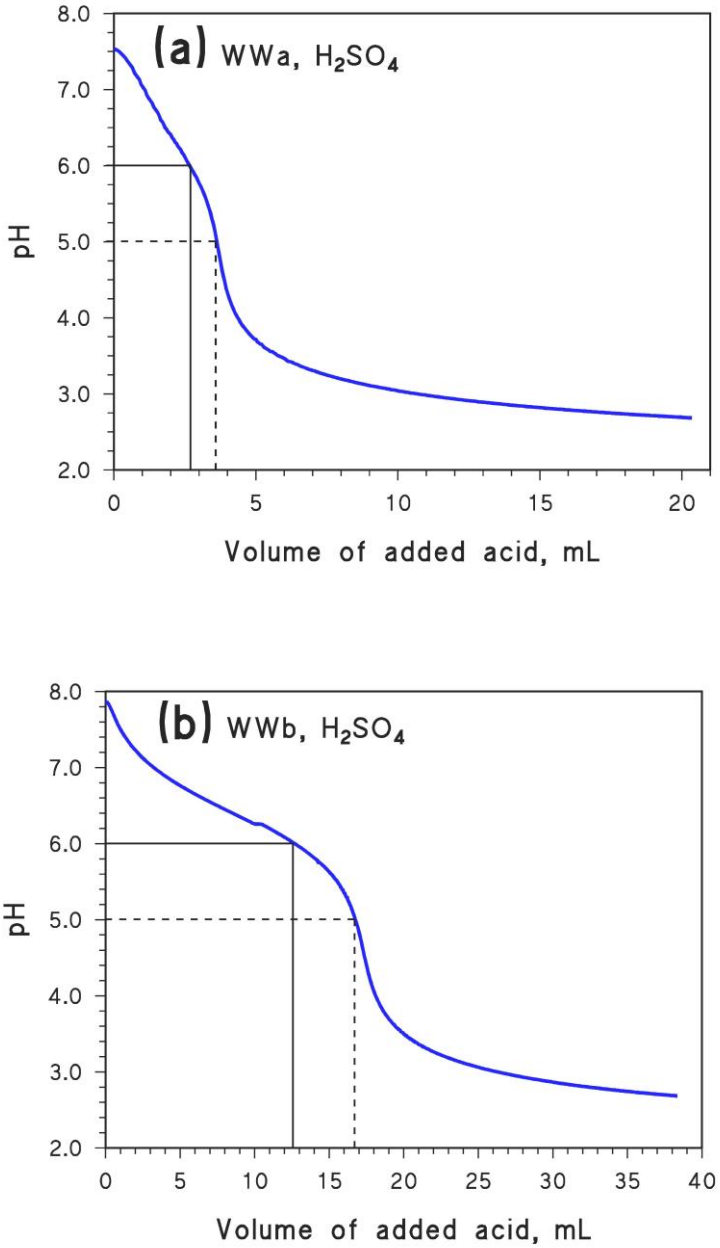

Figure S7. Acid-base titration results of the wastewater samples (WWa, WWb) with H_2SO_4 and H_3PO_4. **(a)** Titration of WWa with 4.5×10^{-3} mol L^{-1} H_2SO_4. **(b)** Titration of WWb with 4.5×10^{-3} mol L^{-1} H_2SO_4. The volumes of acid needed to fix the wastewater pH to 5 and 6 are highlighted with the dashed and solid lines, respectively.

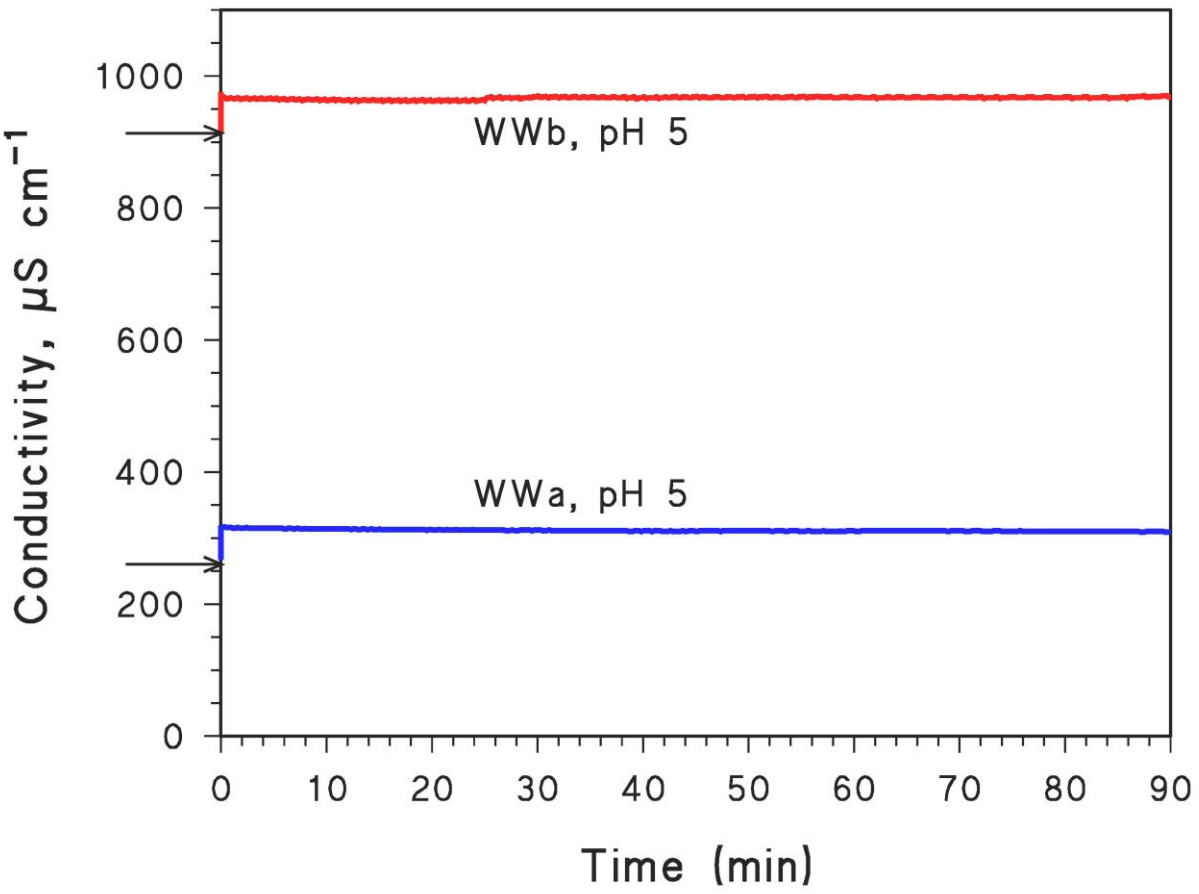

Figure S8. Time trends of conductivity upon degradation of a mixture of 4 µmol L^{-1} CFZ + 4 µmol L^{-1} VNM + 4 µmol L^{-1} IMI in wastewater WWa and WWb. With both wastewaters, the pH 5 was adjusted initially with H_2SO_4 and corrected again at 30 min; ZVI loading was 0.02 g L^{-1}; H_2O_2 concentration was 400 µmol L^{-1}, added in three aliquots (300 µmol L^{-1} at 0 min, 50 µmol L^{-1} at 30 min, and 50 µmol L^{-1} at 60 min). The horizontal arrows highlight the conductivity values of the original wastewater.

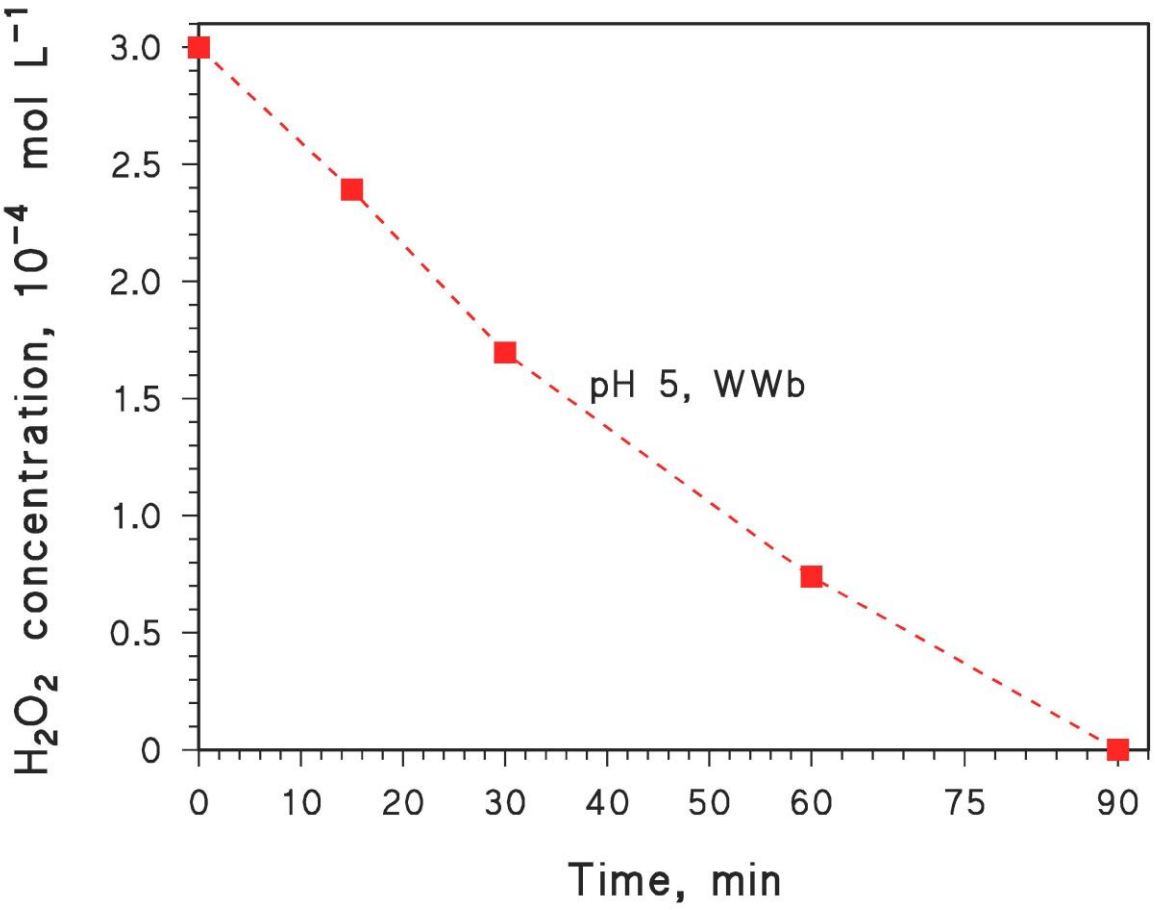

Figure S9. Time trends of H_2O_2 upon degradation of a mixture of 4 µmol L^{-1} CFZ + 4 µmol L^{-1} VNM + 4 µmol L^{-1} IMI in secondary wastewater (WWb) at pH 5 (adjusted initially with H_2SO_4 and corrected again at 30 min). The ZVI loading was 0.02 g L^{-1}; the H_2O_2 concentration was 400 µmol L^{-1}, added in three aliquots (300 µmol L^{-1} at 0 min, 50 µmol L^{-1} at 30 min, and 50 µmol L^{-1} at 60 min).

Table S5. Optimized operational conditions to achieve complete ZVI-Fenton degradation of CFZ, IMI and VNM in mixture (the initial concentration of each antibiotic was 4 μmol L^{-1}) in both wastewaters (WWa, WWb), at pH 5 with H_2SO_4.

Time, min	**ZVI + H_2O_2**
	H_2SO_4, pH 5
0	H_2O_2 3×10^{-4} M
	ZVI 0.02 g L^{-1}
30	H_2O_2 5×10^{-5} M
	Correct pH to 5
60	H_2O_2 5×10^{-5} M
90	End
Notes	*Final pH of 5.7-5.8*

Table S6. Proposed chemical structures of the quasi-molecular ion $[M+H]^+$ and of three corresponding product ions of each antibiotic investigated and the transformation intermediates, with their retention times (RT)

Compound	RT (min)	Precursor Ion $[M+H]^+$	Product Ion 1	Product Ion 2	Product Ion 3
CFZ	12.43	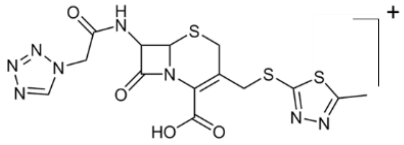 *m/z* 455.1	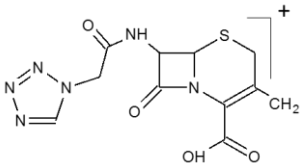 *m/z* 323.1	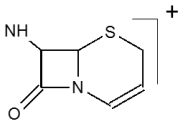 *m/z* 156.1	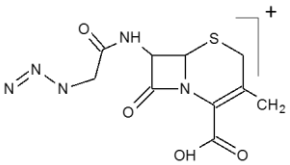 *m/z* 295.1
CFZ-P1a	1.51	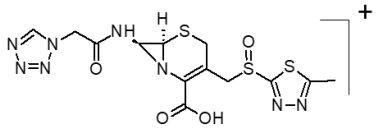 *m/z* 442.8	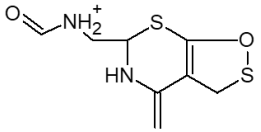 *m/z* 231.0	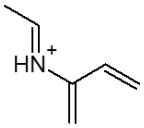 *m/z* 96.0	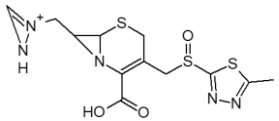 *m/z* 372.3
CFZ-P1b	1.84	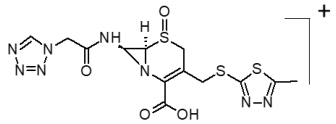 *m/z* 442.8	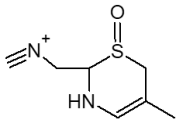 *m/z* 171.0	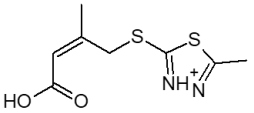 *m/z* 231	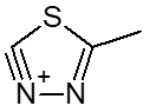 *m/z* 99.0
CFZ-P1c	11.80	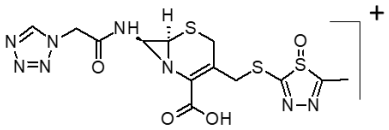 *m/z* 442.8	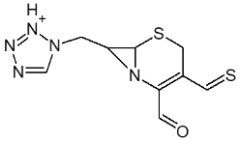 *m/z* 268	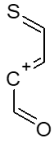 *m/z* 98	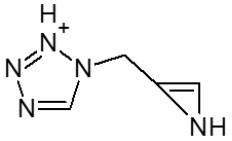 *m/z* 124
CFZ-P2a	2.98	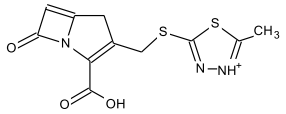 *m/z* 296.1	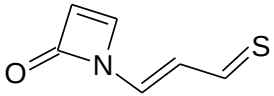 m/z 140	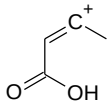 m/z 85	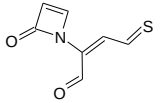 m/z 168
CFZ-P2b	4.02	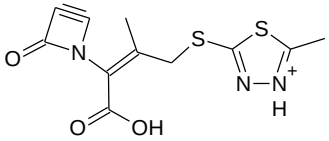 *m/z* 296.1	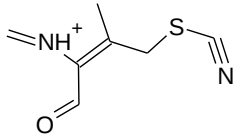 *m/z* 169	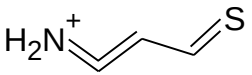 *m/z* 86	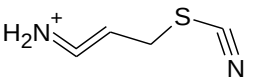 *m/z* 113

CFZ-P3a	1.08	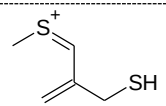 *m/z* 133.0	 *m/z* 72.9	 *m/z* 56.8	 *m/z* 86.9
CFZ-P3b	6.31	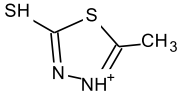 *m/z* 133.0	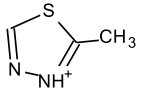 *m/z* 98.9	 *m/z* 58.9	 *m/z* 91.9
CFZ-P4a	7.87	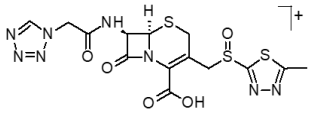 *m/z* 471.0	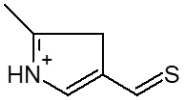 *m/z* 126.0	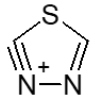 *m/z* 85	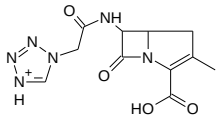 *m/z* 293.0
CFZ-P4b	8.18	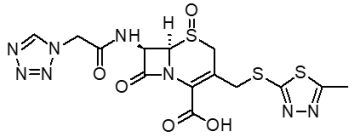 *m/z* 471.0	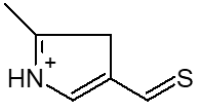 *m/z* 126	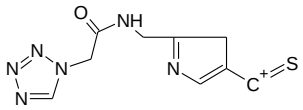 *m/z* 249	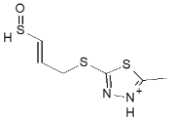 *m/z* 221
CFZ-P5a	9.71	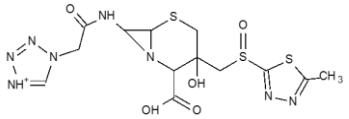 *m/z* 461.0	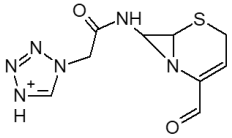 *m/z* 267.0	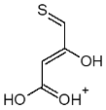 *m/z* 133.0	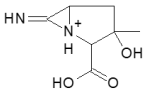 *m/z* 171.0
CFZ-P5b	9.93	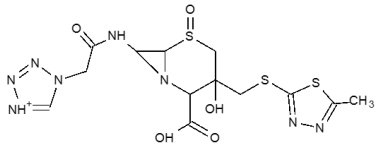 *m/z* 461.0	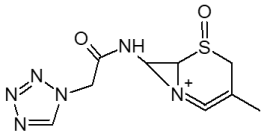 m/z 267.0	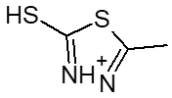 *m/z* 133	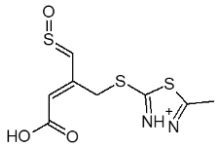 *m/z* 277.0

CFZ-P5d	11.51	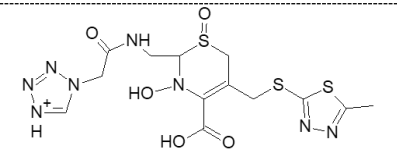 *m/z* 461.0	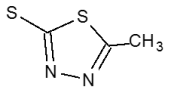 *m/z* 133.0	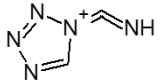 *m/z* 96.0	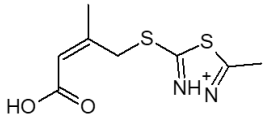 *m/z* 231.0
CFZ-P6a	12.38	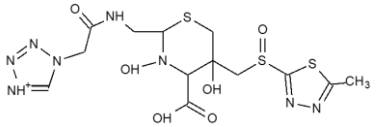 *m/z* 479.0	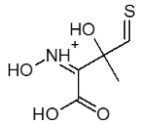 *m/z* 178.0	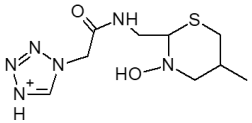 *m/z* 317.1	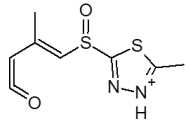 *m/z* 229.0
CFZ-P6b	13.63	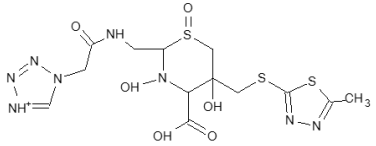 *m/z* 479.0	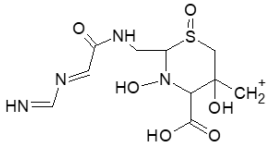 *m/z* 319.0	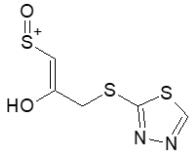 *m/z* 221.2	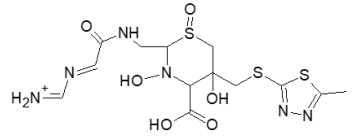 *m/z* 451.1
CFZ-P7	1.31	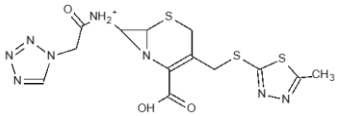 *m/z* 427.0	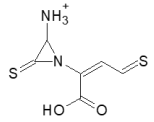 *m/z* 203.0	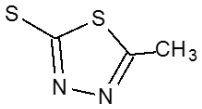 *m/z* 133.0	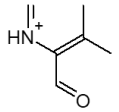 *m/z* 112.0
CFZ-P8a	1.54	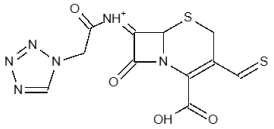 *m/z* 353.0	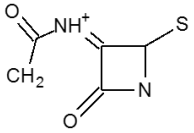 *m/z* 254.9	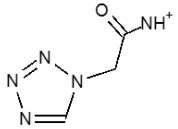 *m/z* 157.0	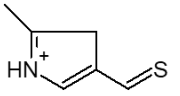 *m/z* 126.0
CFZ-P8b	7.30	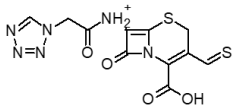 *m/z* 353.0	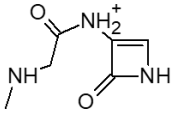 *m/z* 156.0	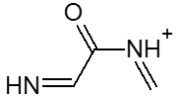 *m/z* 85.0	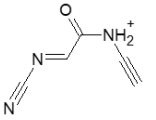 *m/z* 122
IMI	2.17	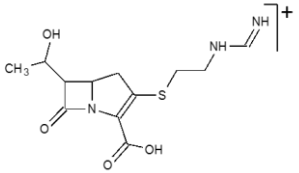 *m/z* 300.1	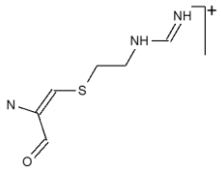 *m/z* 170.0	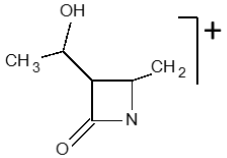 *m/z* 126.07	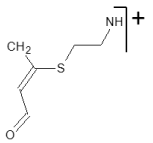 *m/z* 142.03

IMI-P1	3.19	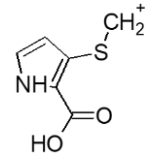 *m/z* 156.0	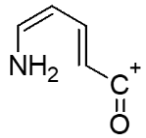 *m/z* 96.0	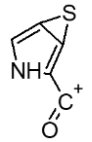 *m/z* 124.0	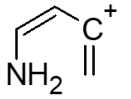 *m/z* 68.0
IMI-P2	2.54	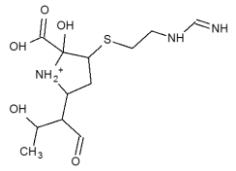 *m/z* 320.1	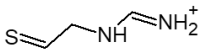 *m/z* 103.0	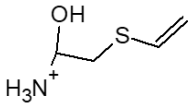 *m/z* 120.0	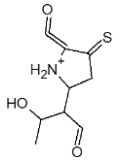 *m/z* 276.1
IMI-P3	7.93	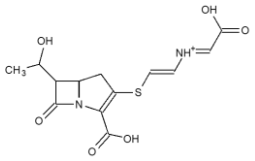 *m/z* 327.1	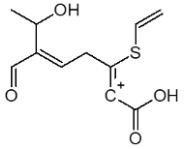 *m/z* 241.0	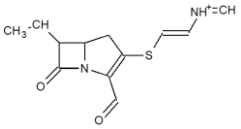 *m/z* 277.0	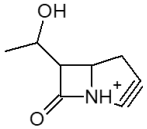 *m/z* 152.1
IMI-P4	3.25	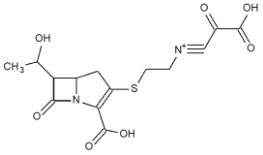 *m/z* 355	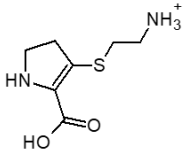 *m/z* 189.1	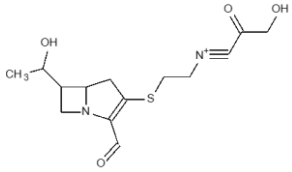 *m/z* 311.1	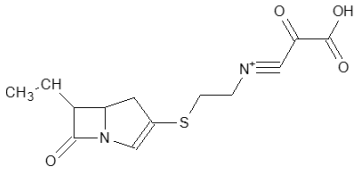 *m/z* 293.0
IMI-P5	8.10	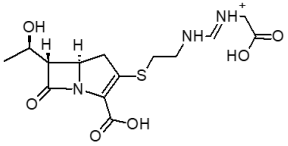 *m/z* 358.0	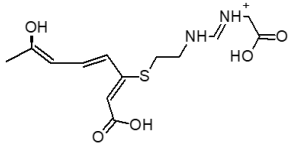 *m/z* 315.1	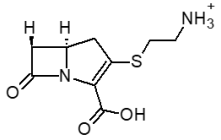 *m/z* 229.0	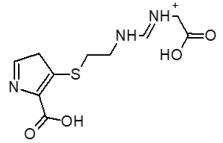 *m/z* 272.0
VNM	3.03	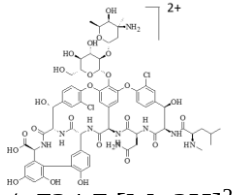 *m/z* 724.7 $[M+2H]^{2+}$	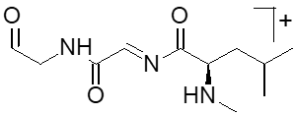 *m/z* 242.2	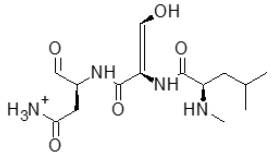 *m/z* 329.0	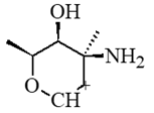 *m/z* 144.0

VNM-P1	7.71	$[M\text{-}OH+H]^{2+}$ *m/z* 715.6	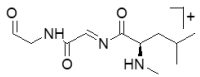 *m/z* 242.2	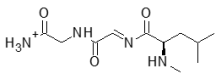 *m/z* 329.0	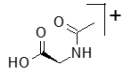 *m/z* 118.0
VNM-P2	5.50	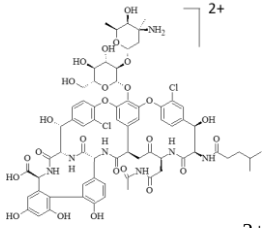 *m/z* 731.2 $[M+2H]^{2+}$	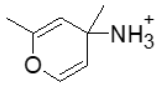 m/z 126.1	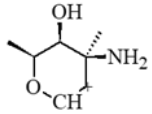 m/z 144.2	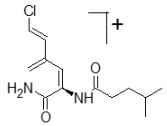 m/z 271.2
VNM-P3	6.05	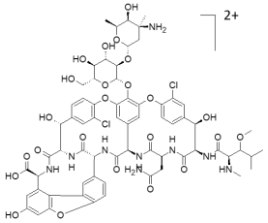 *m/z* 730.7	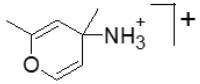 *m/z* 126.0	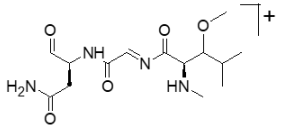 *m/z* 329.1	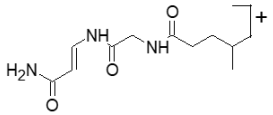 *m/z* 242.2
VNM-P4a	2.06	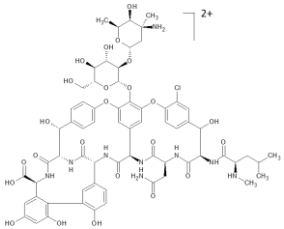 *m/z* 707.8	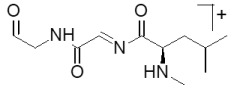 *m/z* 242.2	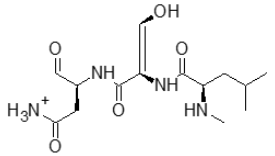 *m/z* 329.2	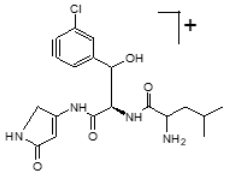 *m/z* 407.2
VNM-P4b	2.55	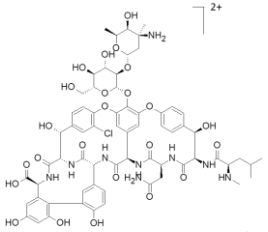 *m/z* 707.8 $[M+2H]^{2+}$	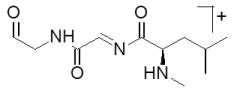 *m/z* 242.2	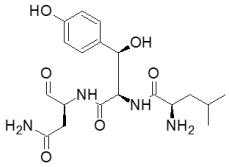 *m/z* 409.2	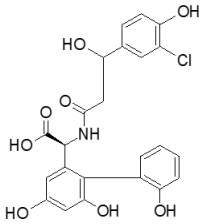 *m/z* 474.1

VNM-P5a	7.34	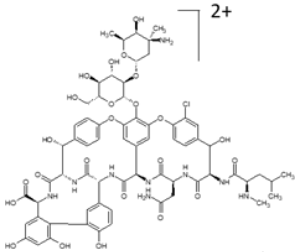 *m/z* 708.2 $[M+2H]^{2+}$	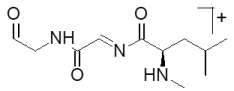 *m/z* 242.1	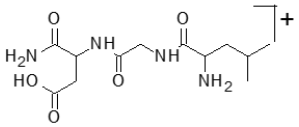 *m/z* 303.1	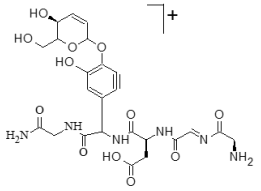 *m/z* 593.2
VNM-P5b	7.40	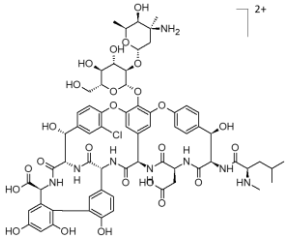 *m/z* 708.2 $[M+2H]^{2+}$	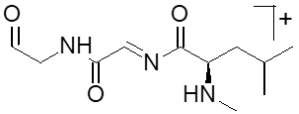 *m/z* 242.1	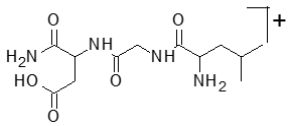 *m/z* 303.1	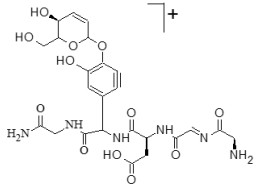 *m/z* 593.2
VNM-P6a	2.40	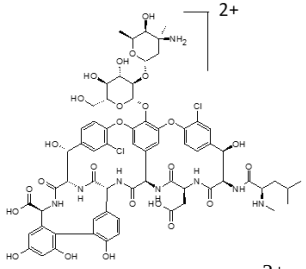 *m/z* 725.2 $[M+2H]^{2+}$	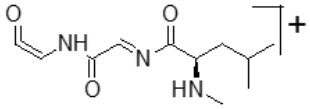 m/z 240.1	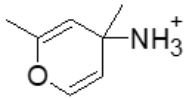 m/z 126.0	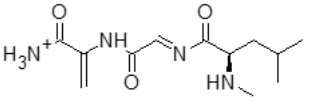 m/z 269.2
VNM-P6b	4.23	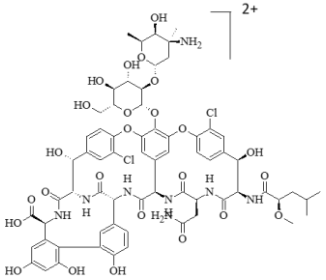 *m/z* 725.2 $[M+2H]^{2+}$	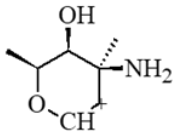 m/z 144.2	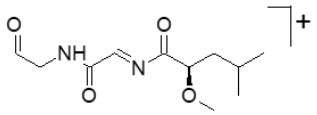 m/z 243.2	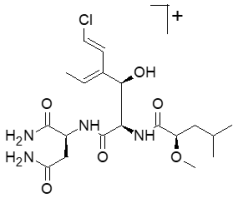 m/z 447.2

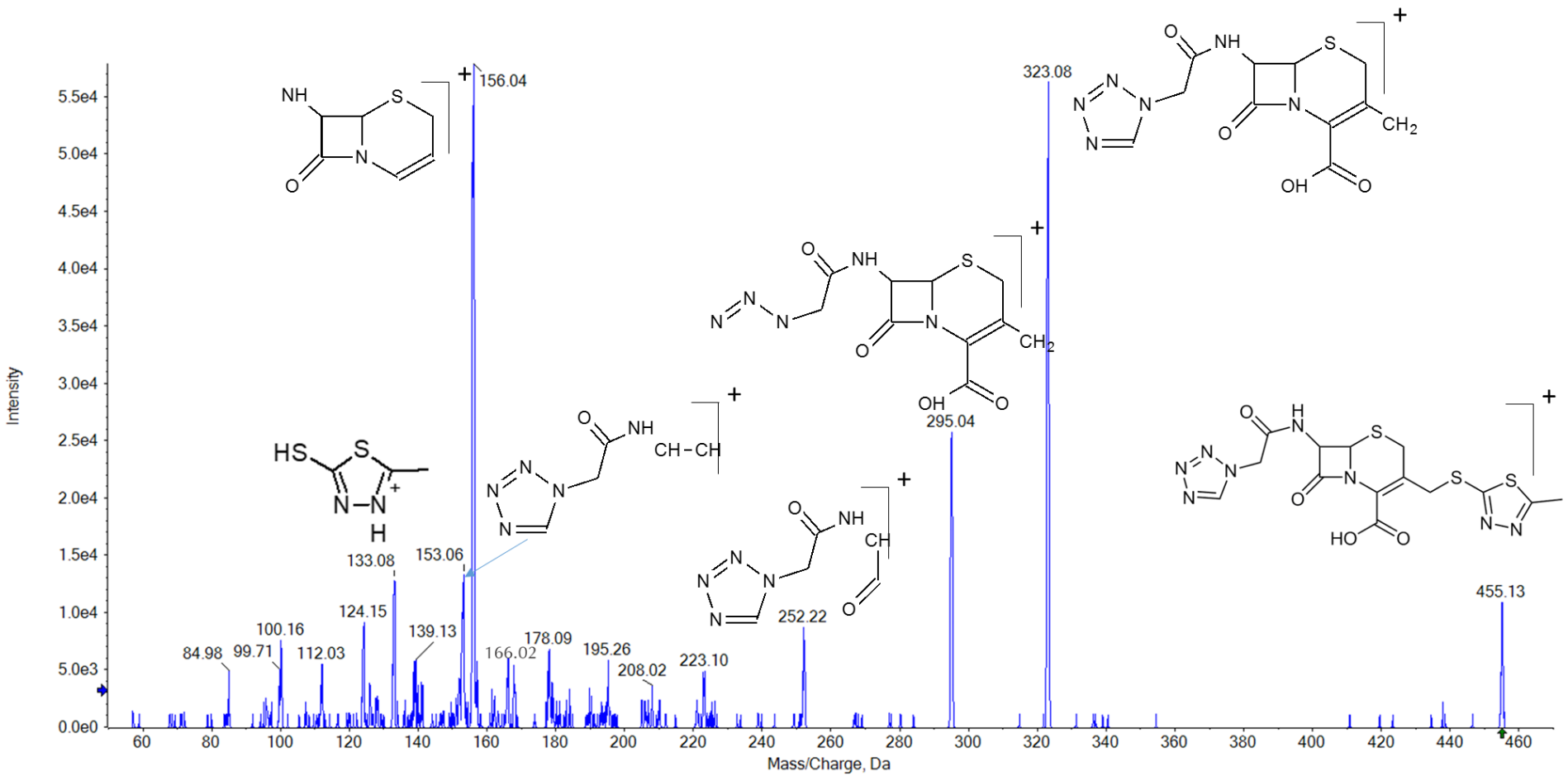

Figure S10. ESI (PI) MS/MS spectrum of CFZ.

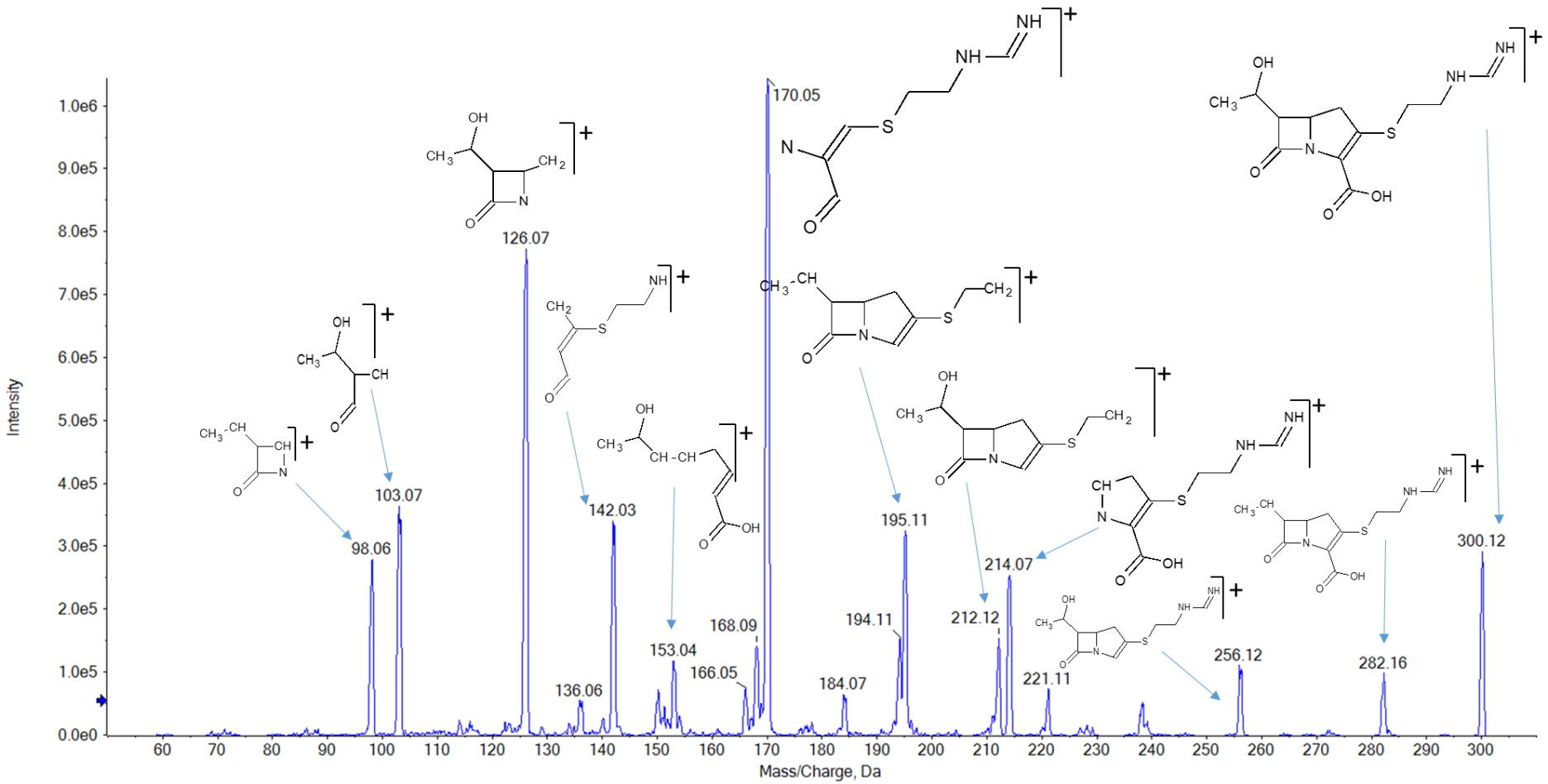

Figure S11. ESI (PI) MS/MS spectrum of IMI.

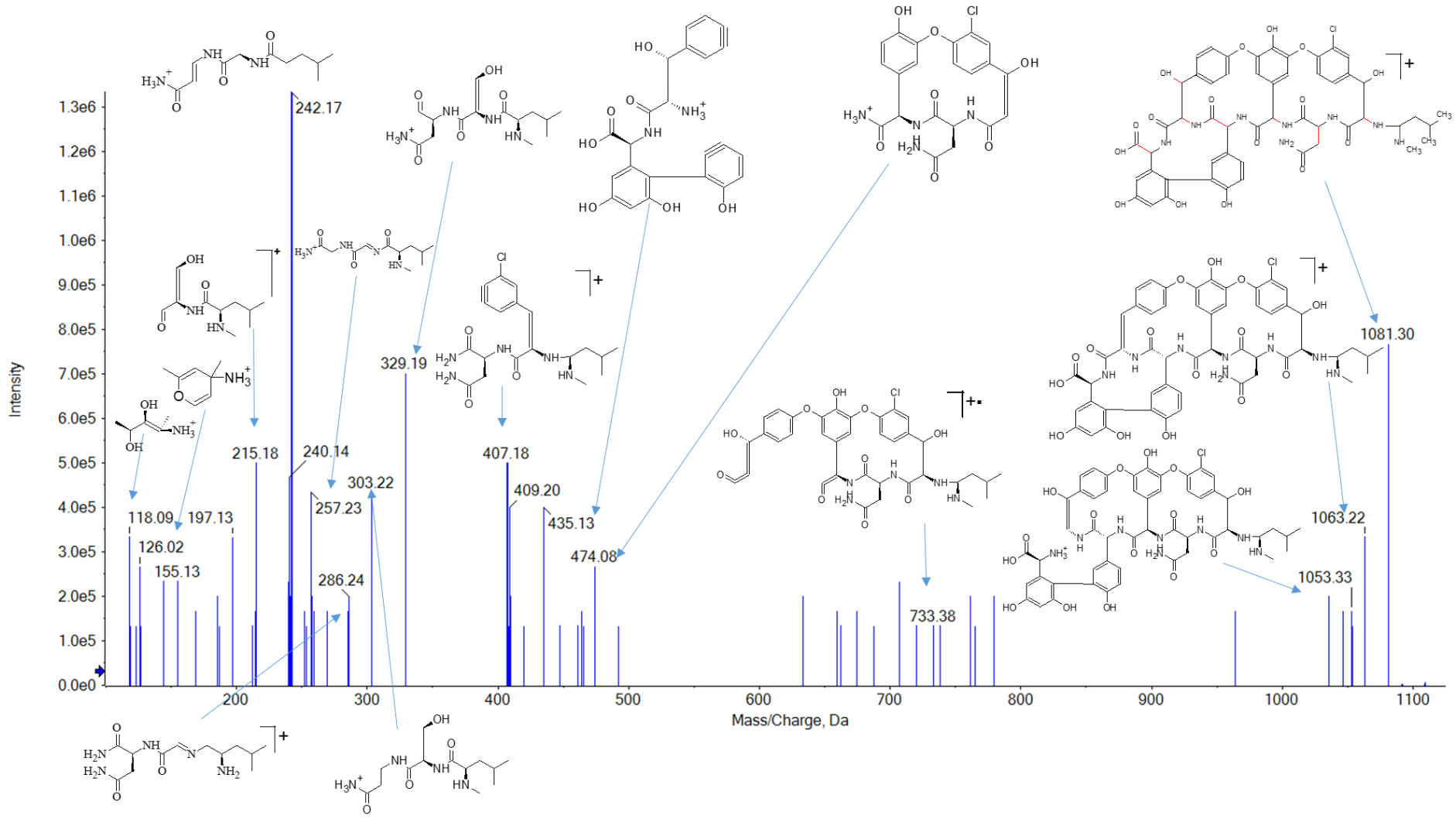

Figure S12. ESI (PI) MS/MS spectrum of VNM.

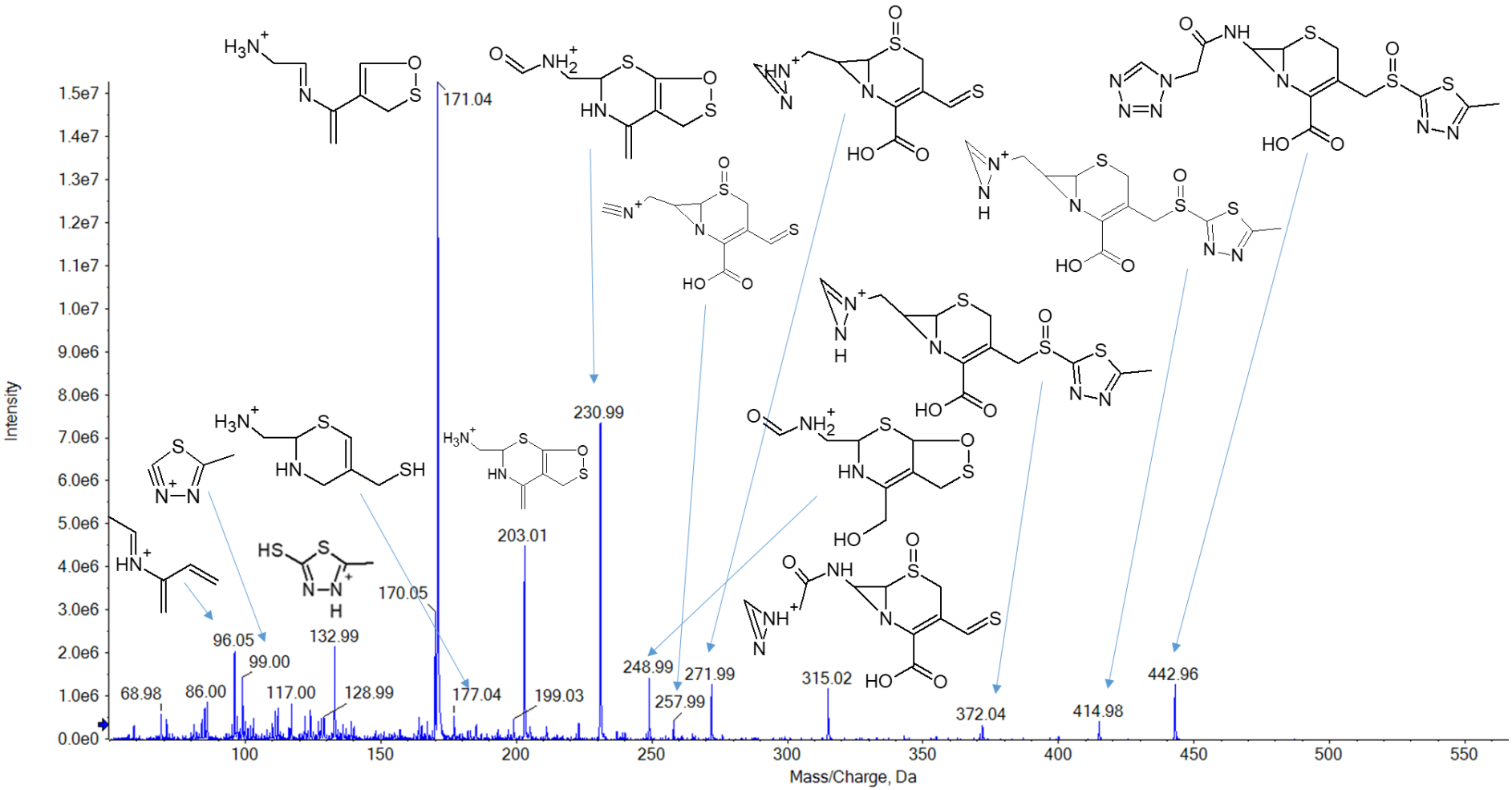

Figure S13. ESI (PI) MS/MS spectrum of CFZ-P1a.

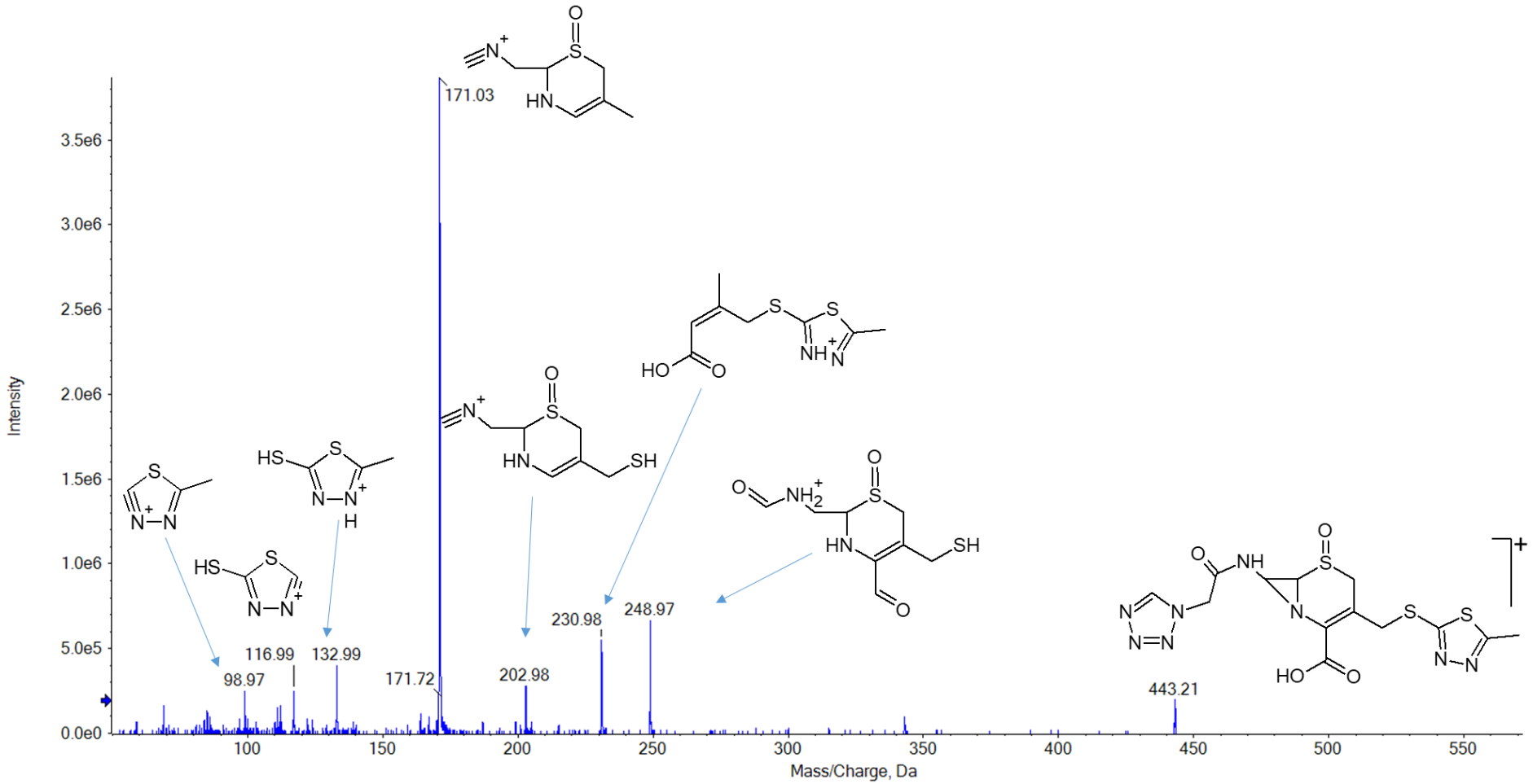

Figure S14. ESI (PI) MS/MS spectrum of CFZ-P1b.

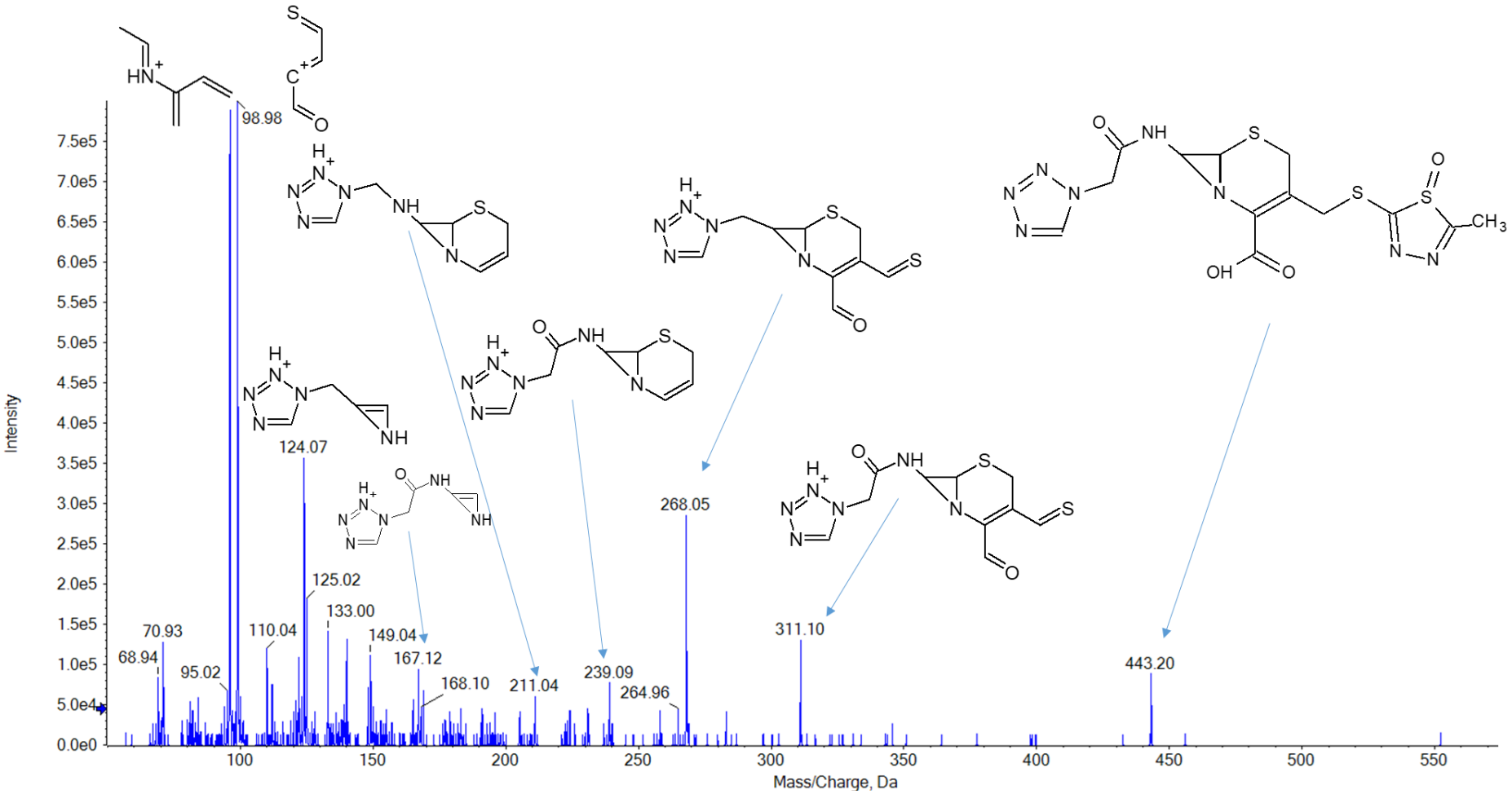

Figure S15. ESI (PI) MS/MS spectrum of CFZ-P1c.

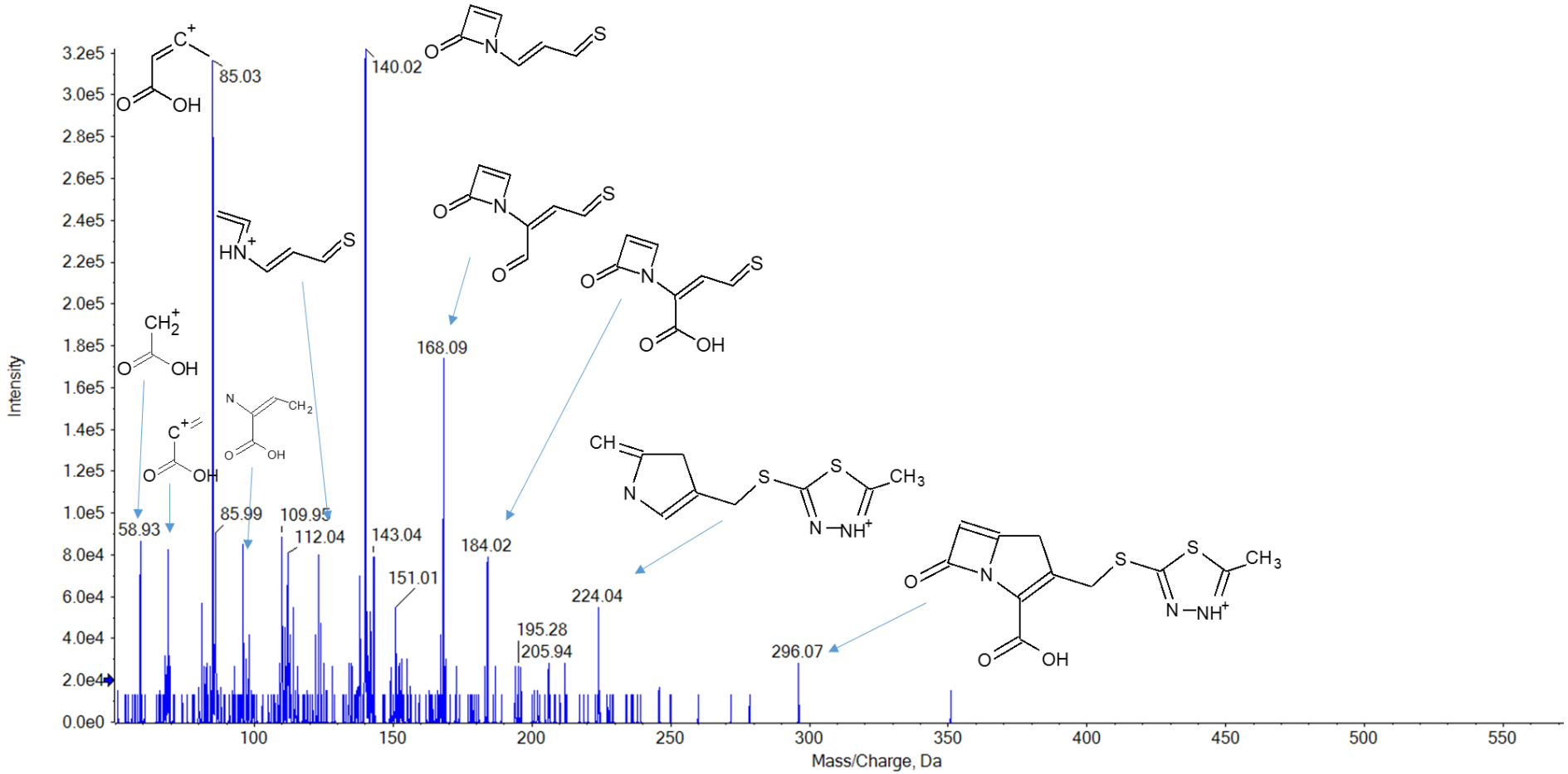

Figure S16. ESI (PI) MS/MS spectrum of CFZ-P2a.

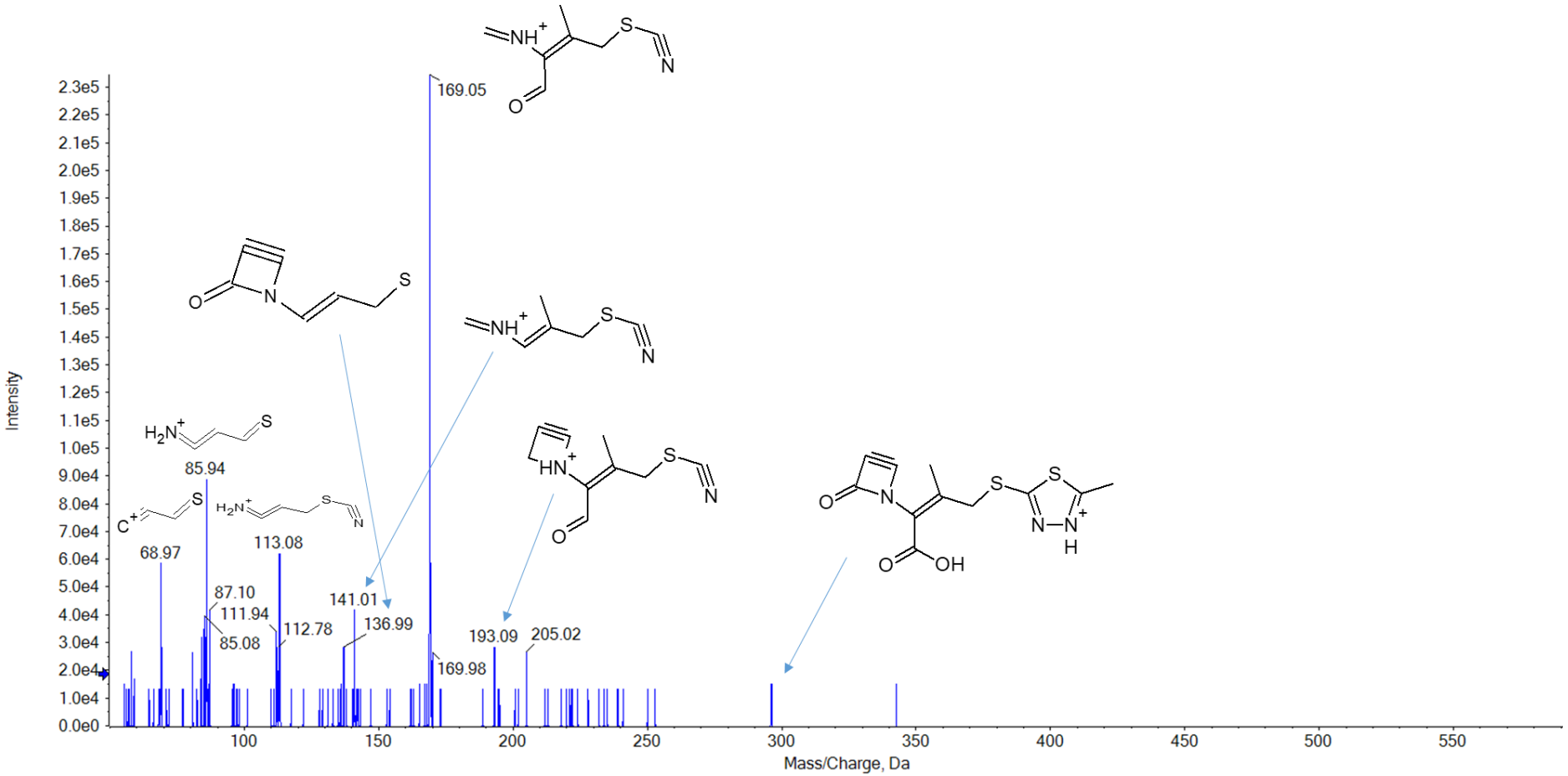

Figure S17. ESI (PI) MS/MS spectrum of CFZ-P2b.

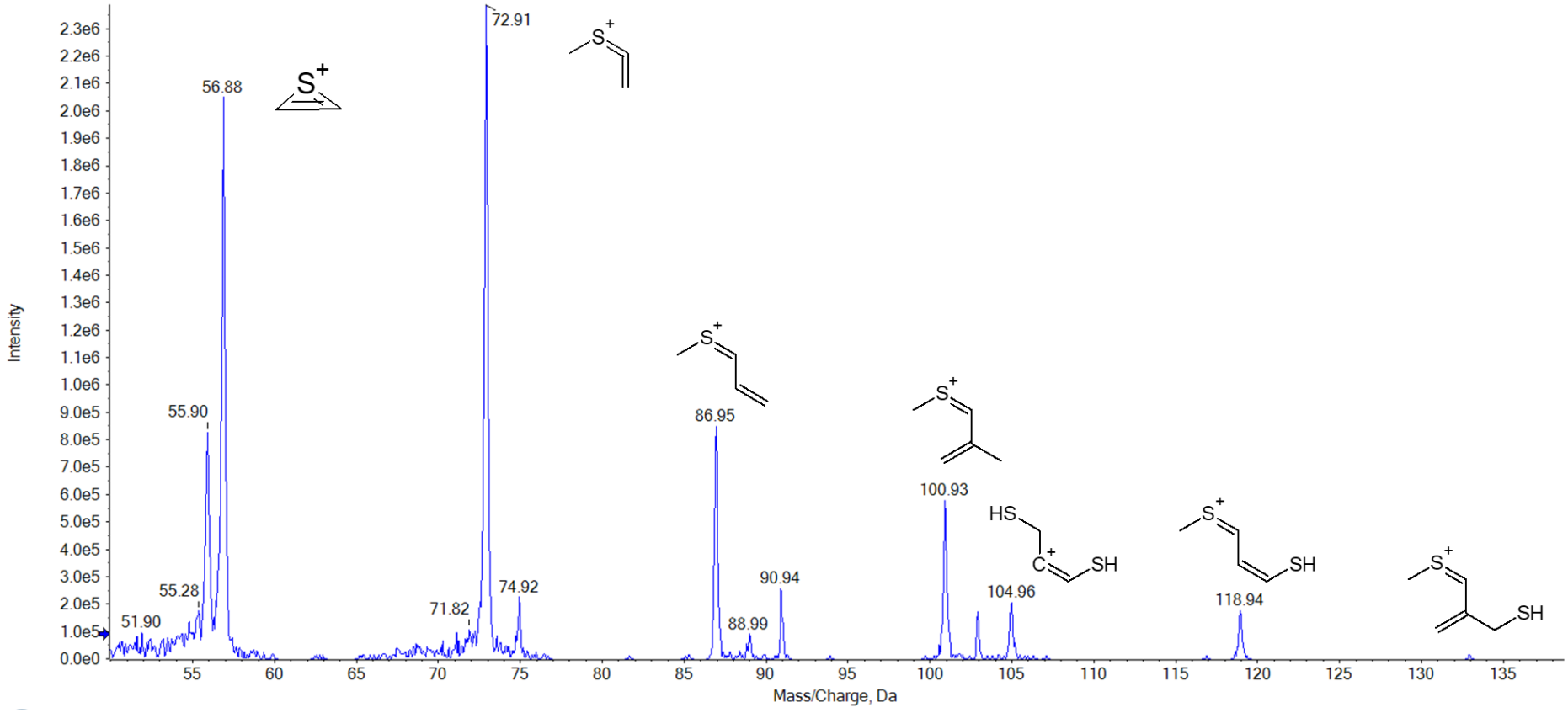

Figure S18. ESI (PI) MS/MS spectrum of CFZ-P3a.

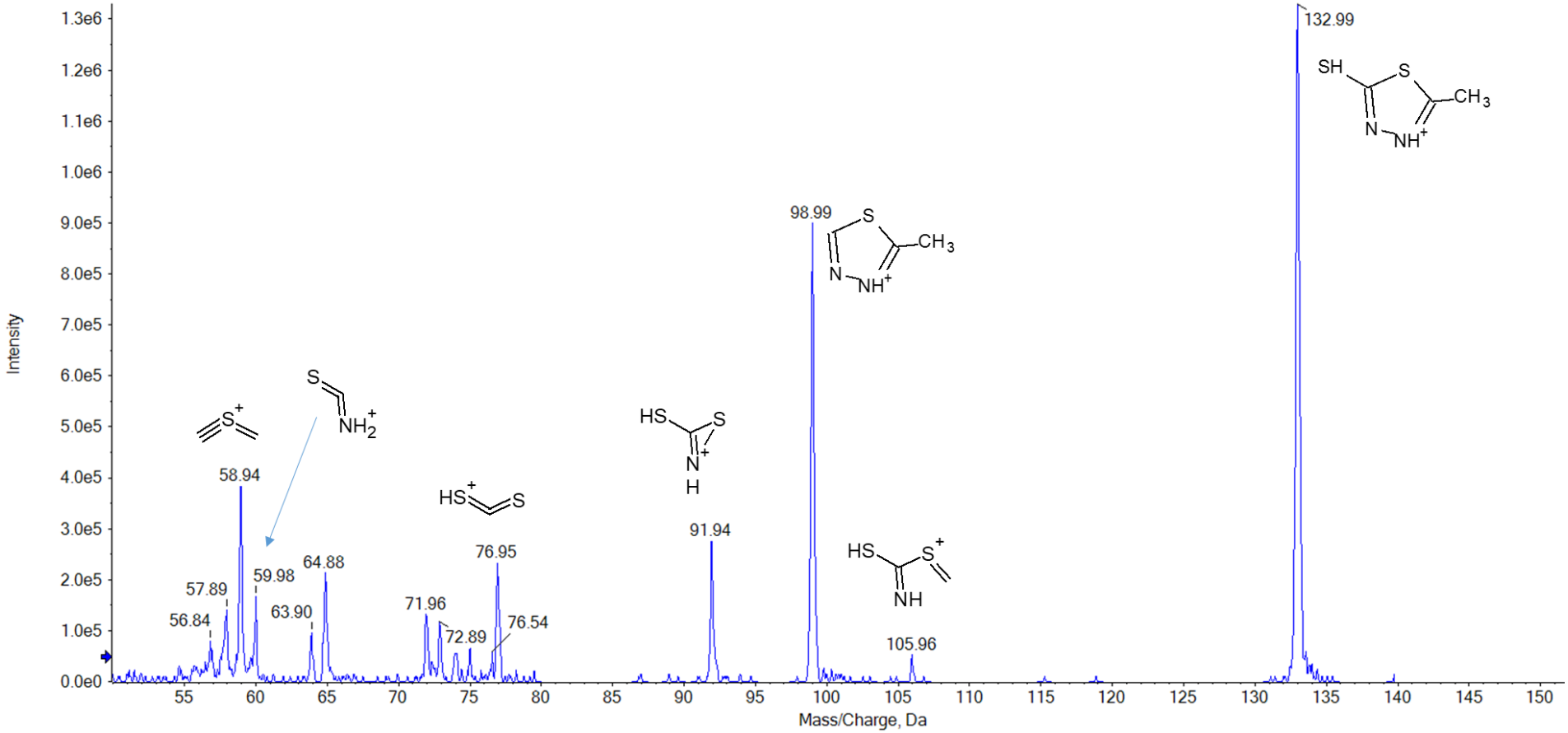

Figure S19. ESI (PI) MS/MS spectrum of CFZ-P3b.

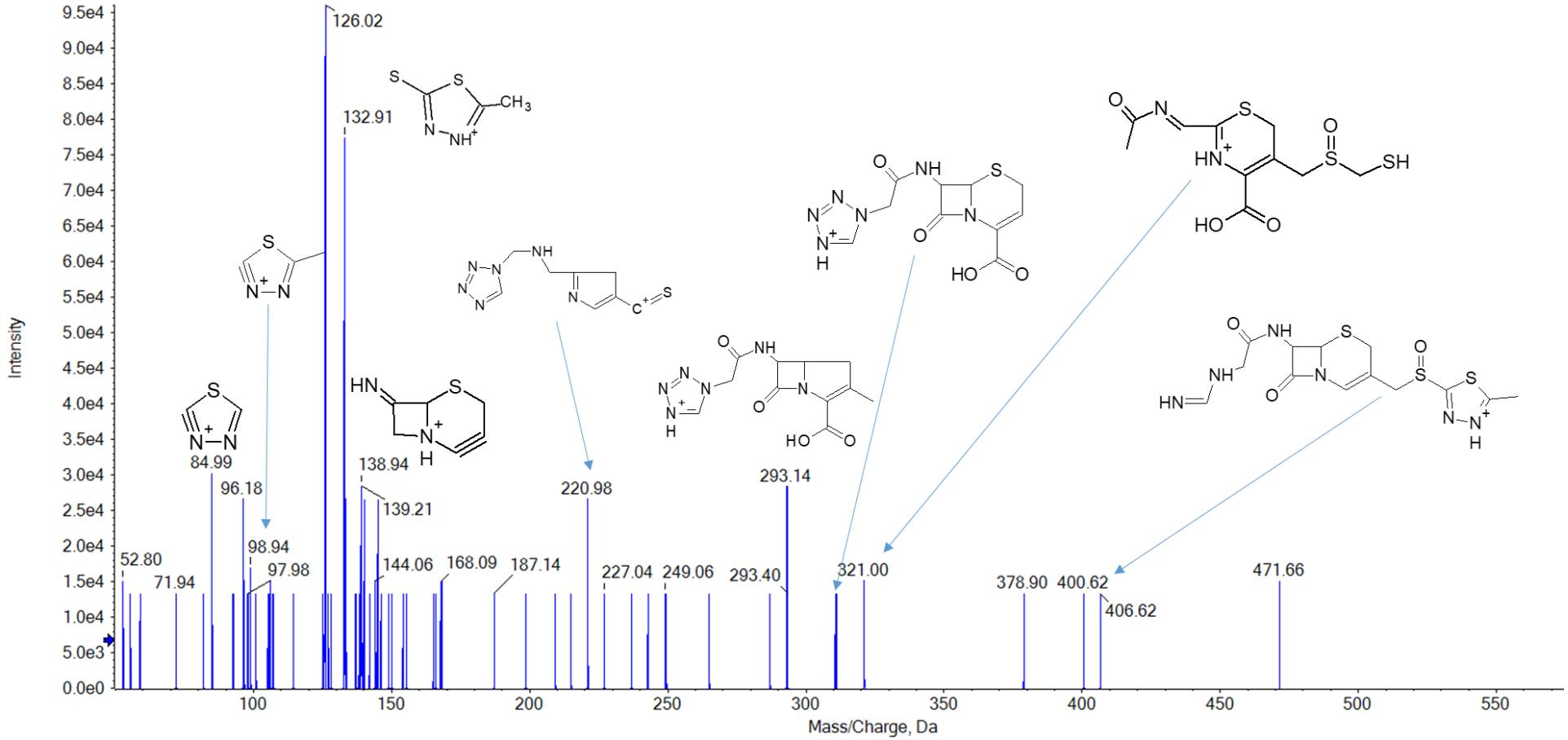

Figure S20. ESI (PI) MS/MS spectrum of CFZ-P4a.

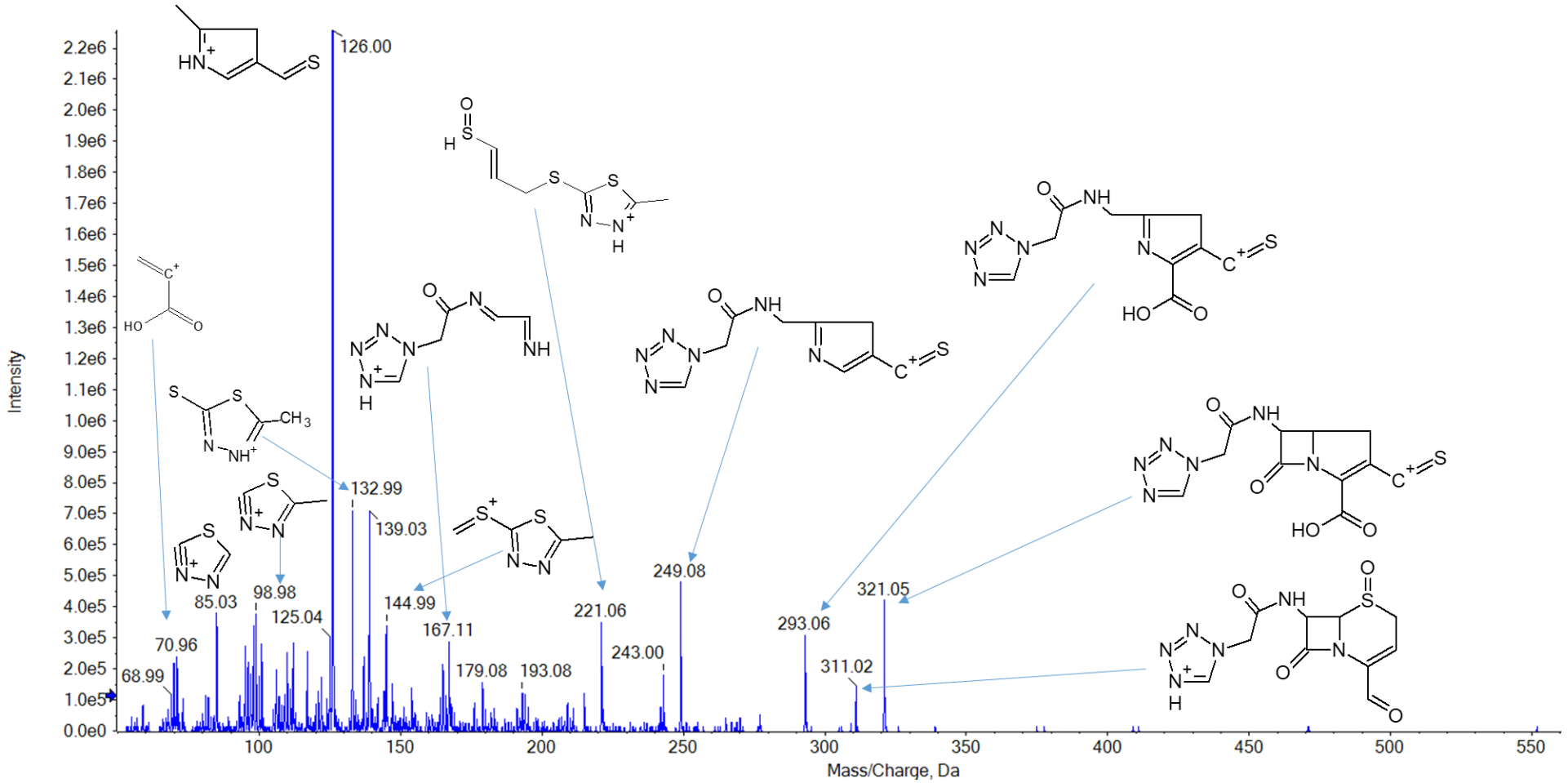

Figure S21. ESI (PI) MS/MS spectrum of CFZ-P4b.

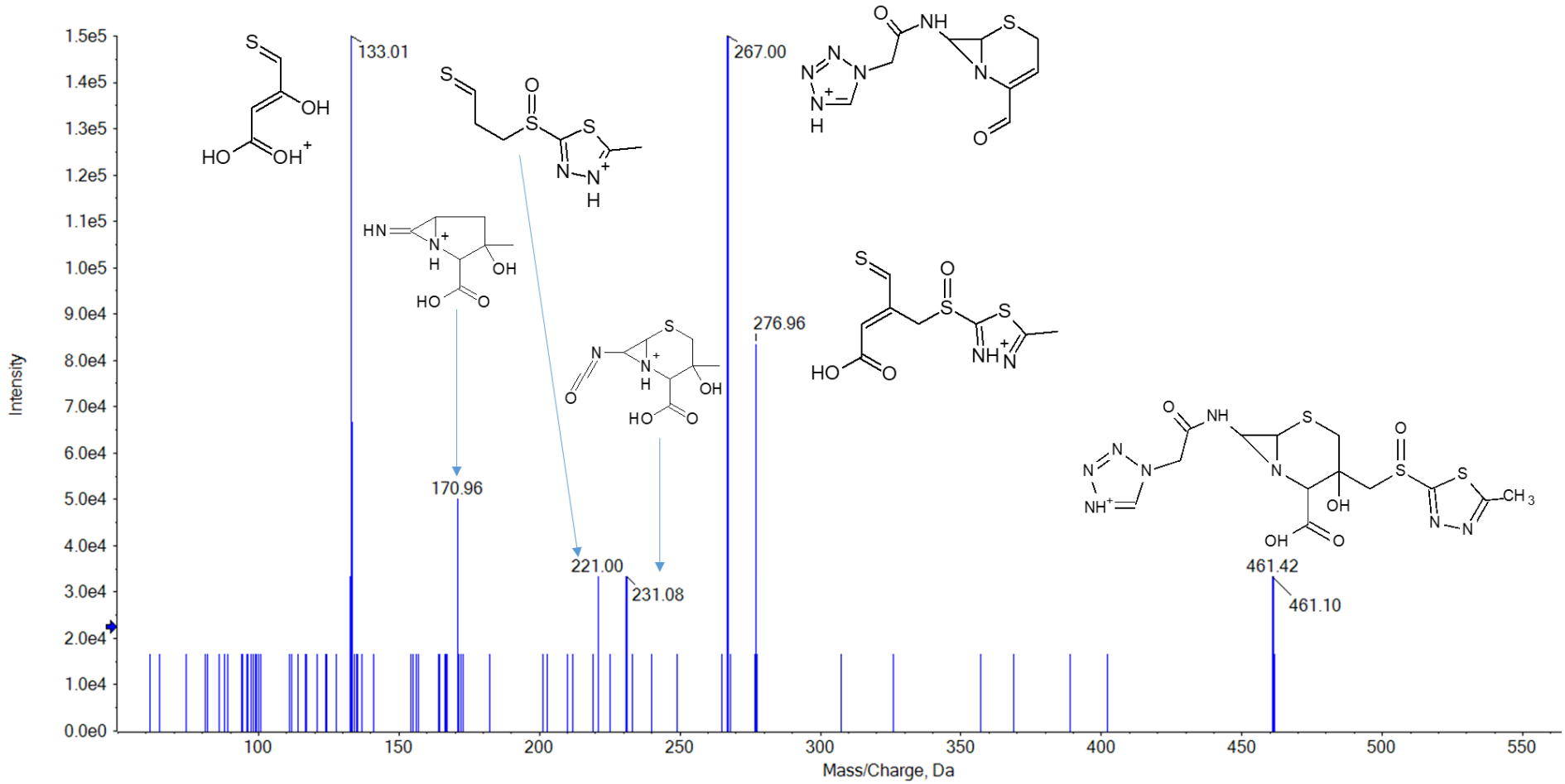

Figure S22. ESI (PI) MS/MS spectrum of CFZ-P5a.

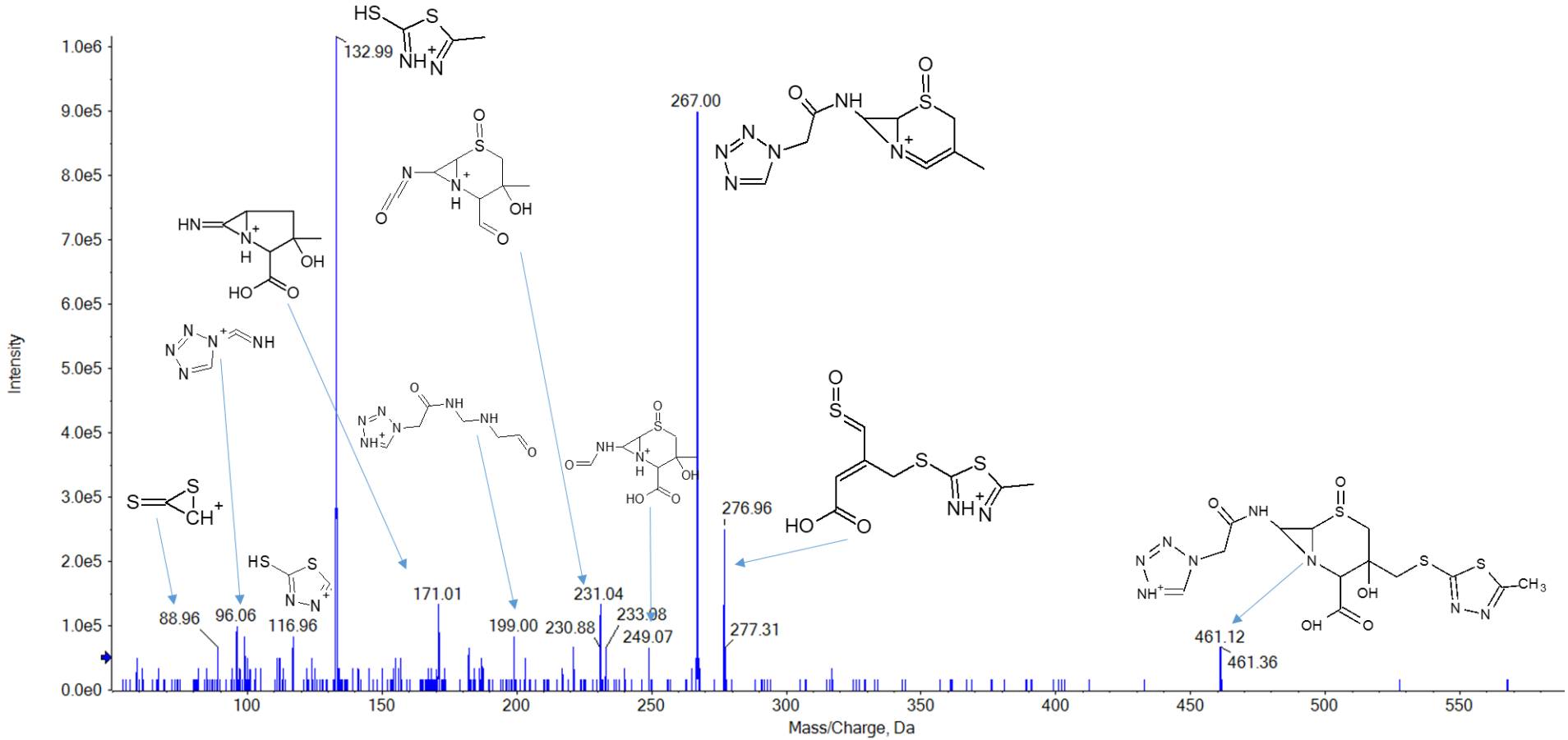

Figure S23. ESI (PI) MS/MS spectrum of CFZ-P5b.

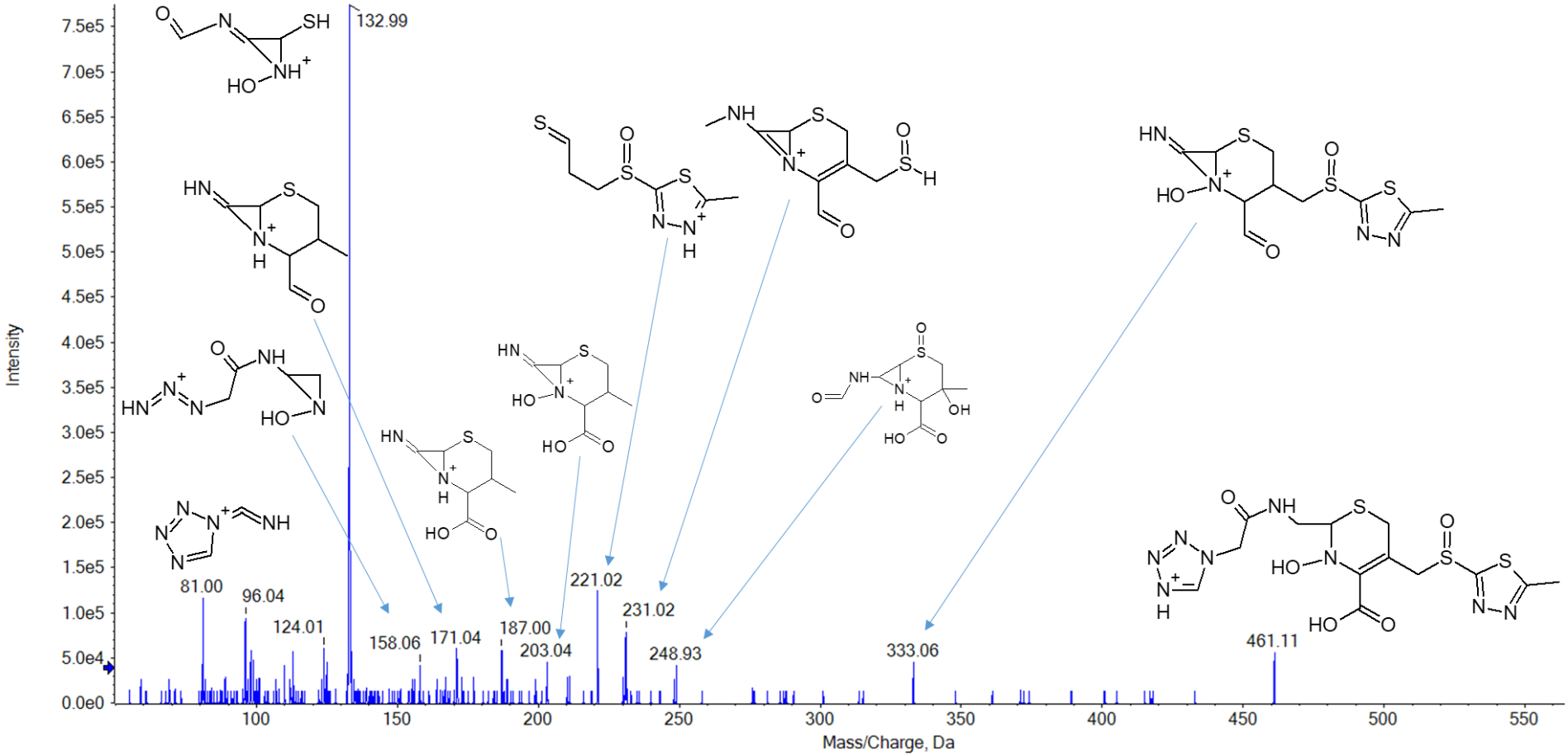

Figure S24. ESI (PI) MS/MS spectrum of CFZ-P5c.

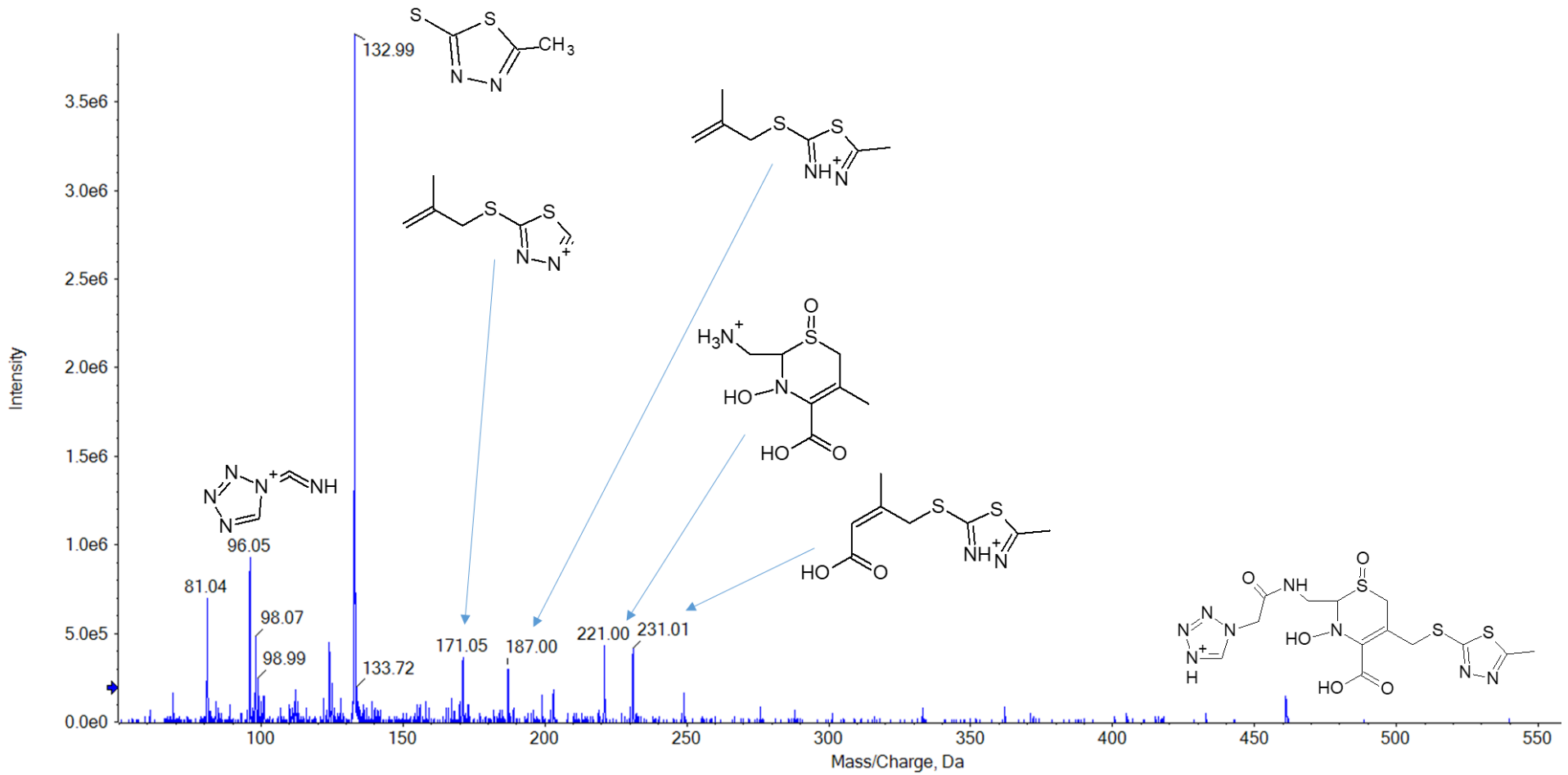

Figure S25. ESI (PI) MS/MS spectrum of CFZ-P5d.

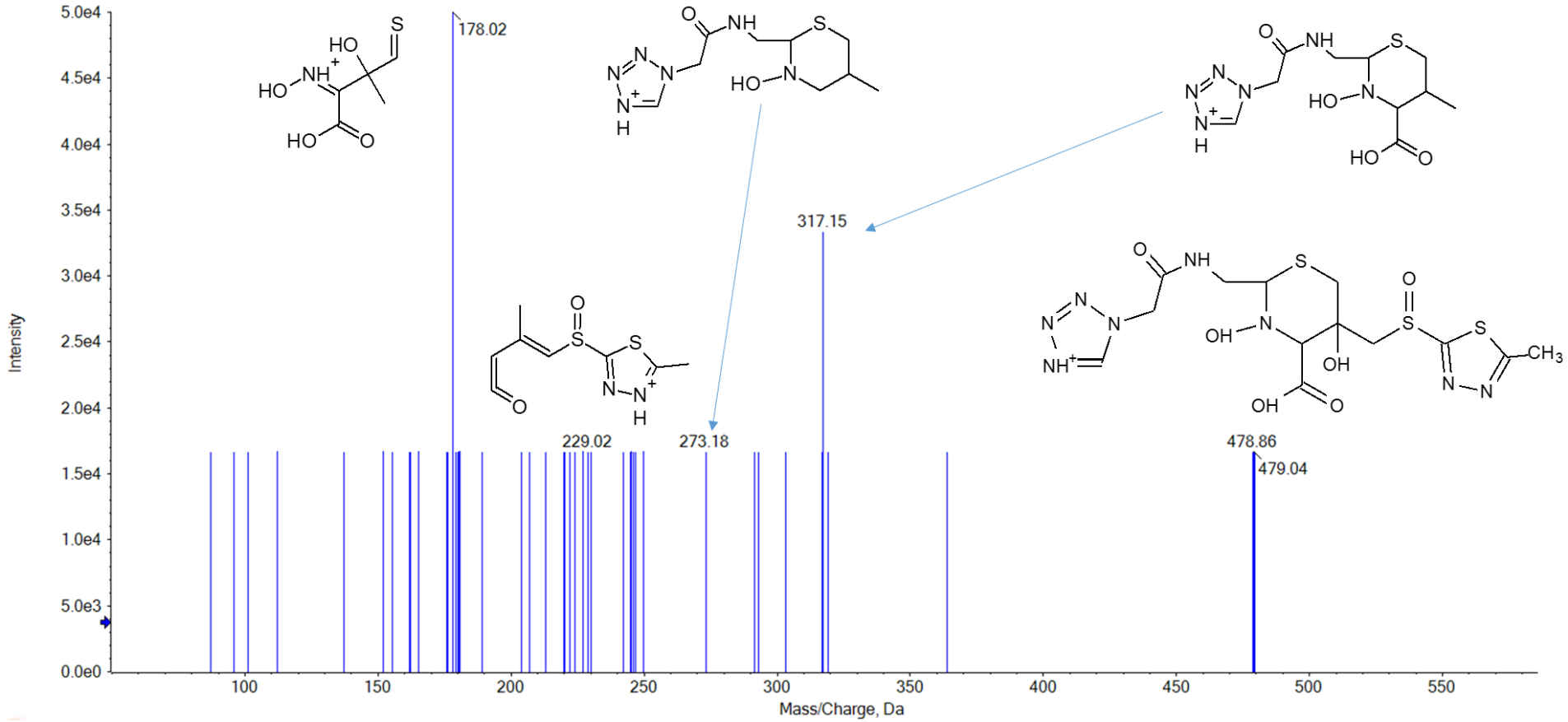

Figure S26. ESI (PI) MS/MS spectrum of CFZ-P6a.

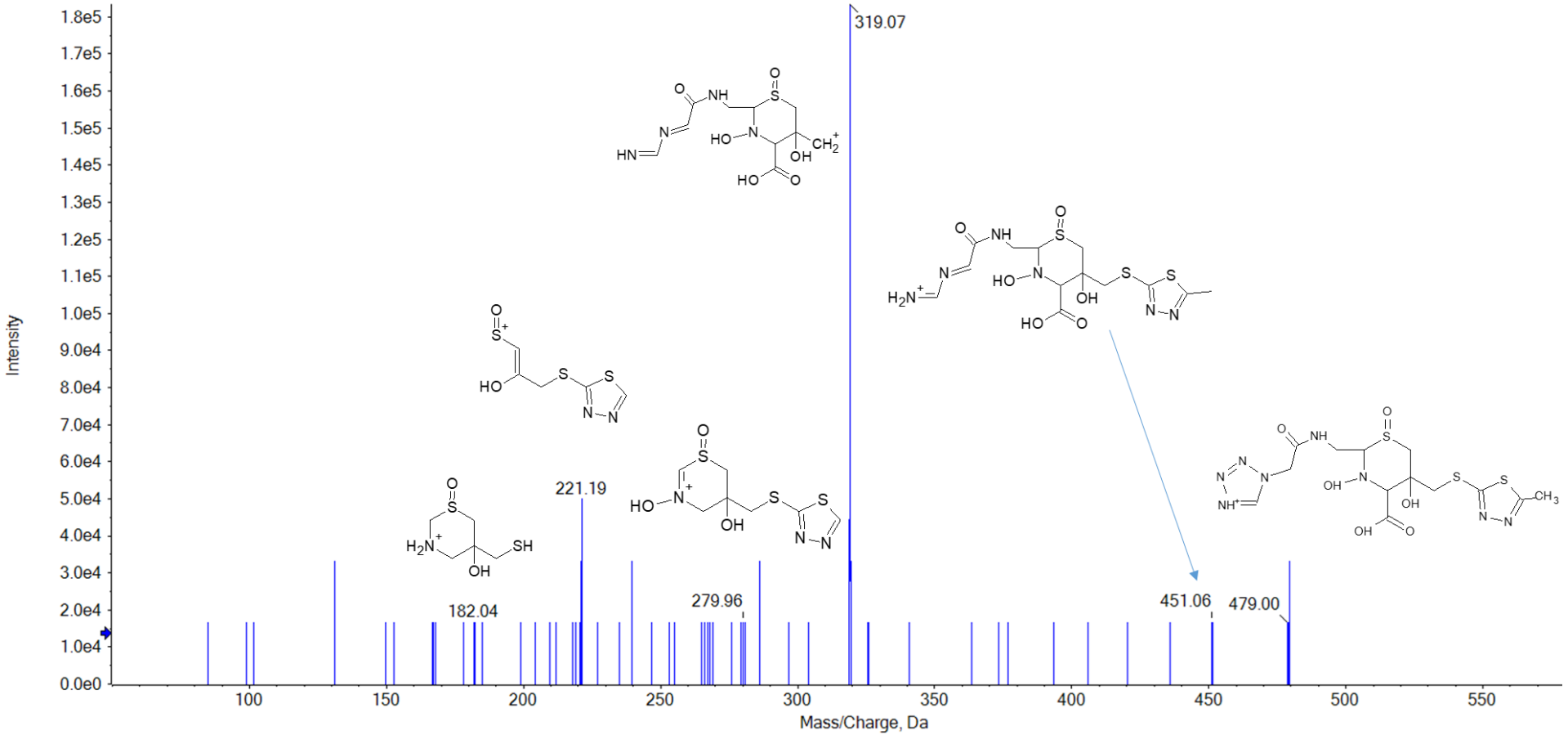

Figure S27. ESI (PI) MS/MS spectrum of CFZ-P6b.

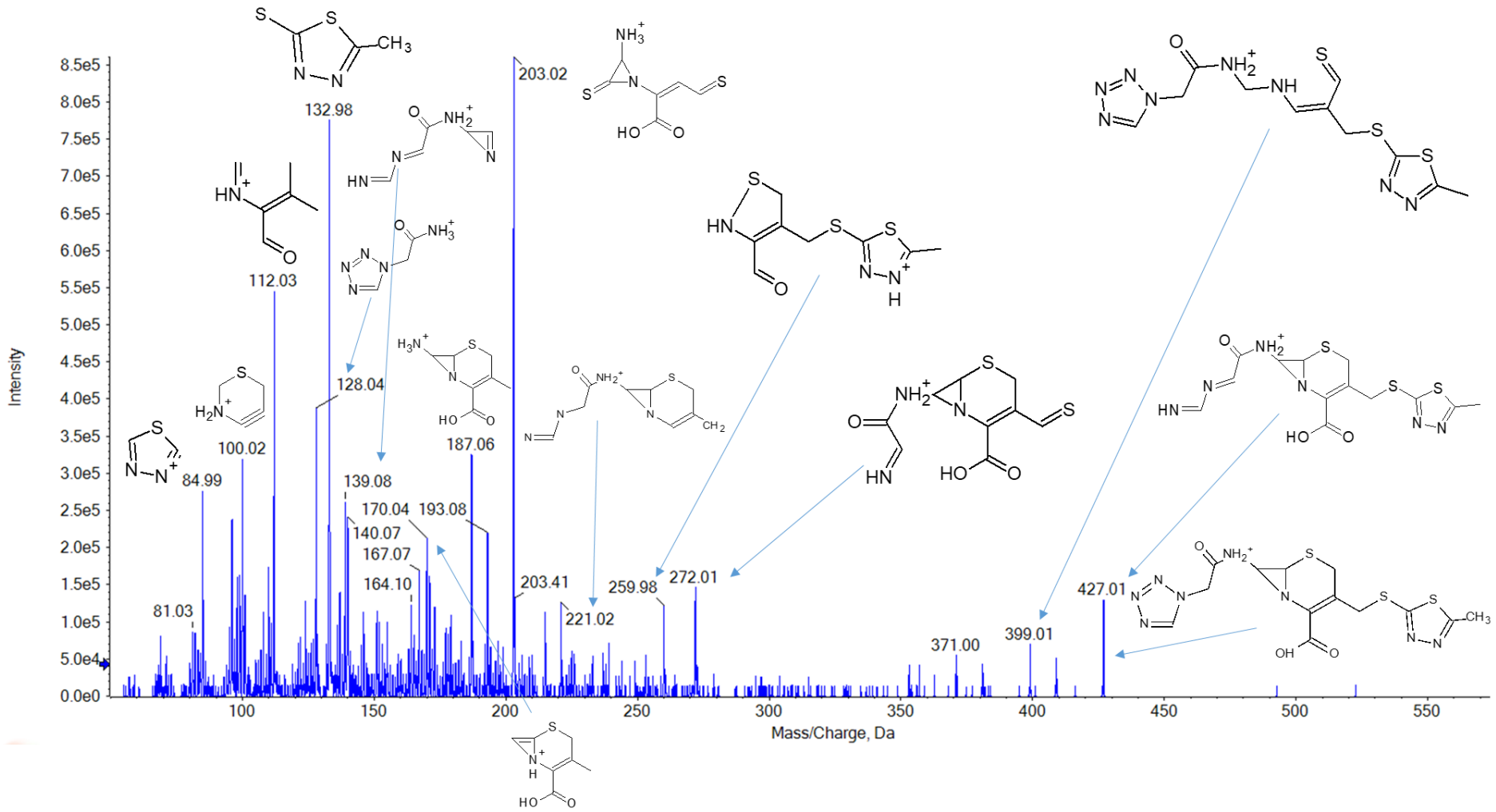

Figure S28. ESI (PI) MS/MS spectrum of CFZ-P7.

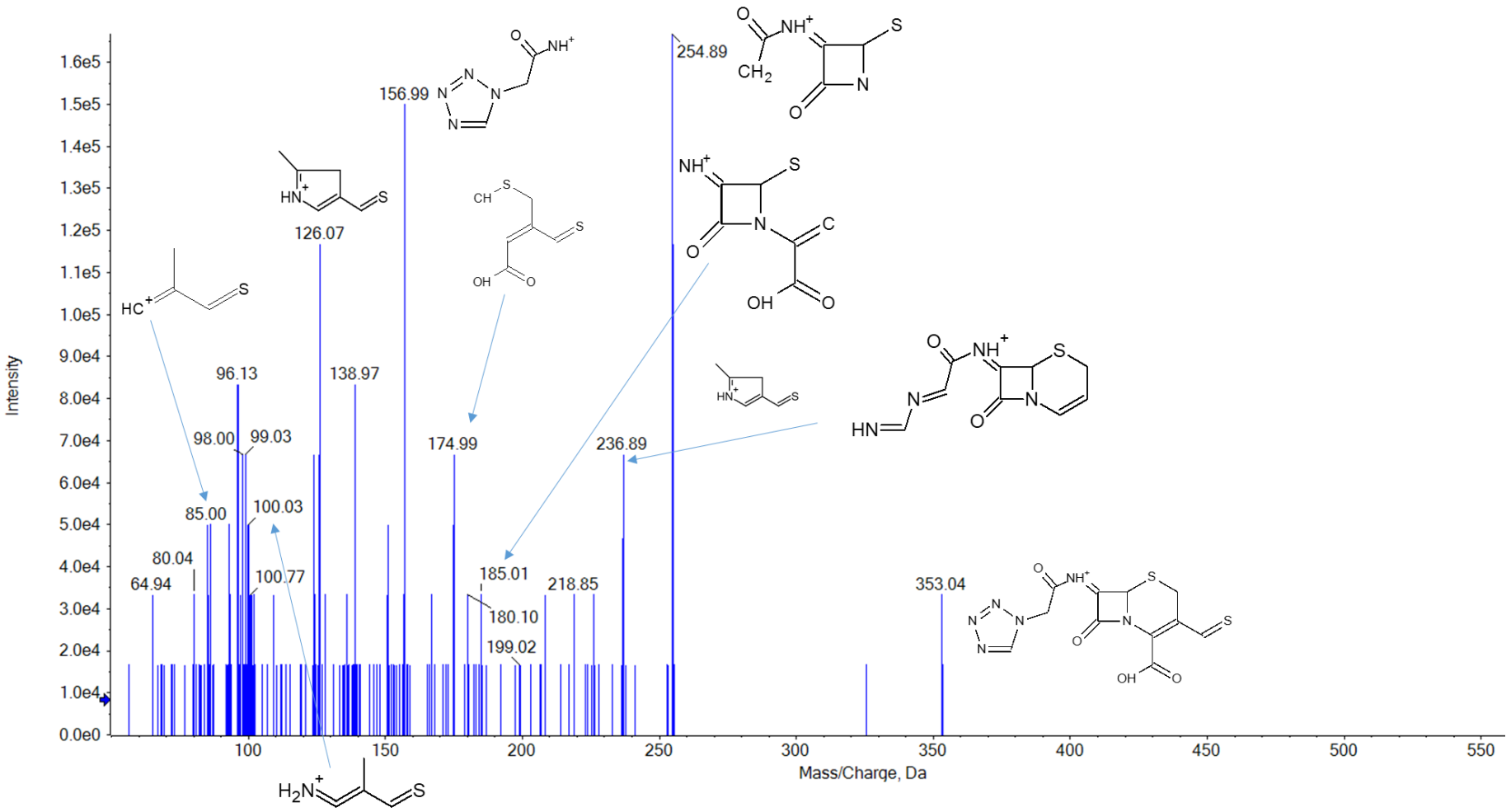

Figure S29. ESI (PI) MS/MS spectrum of CFZ-P8a.

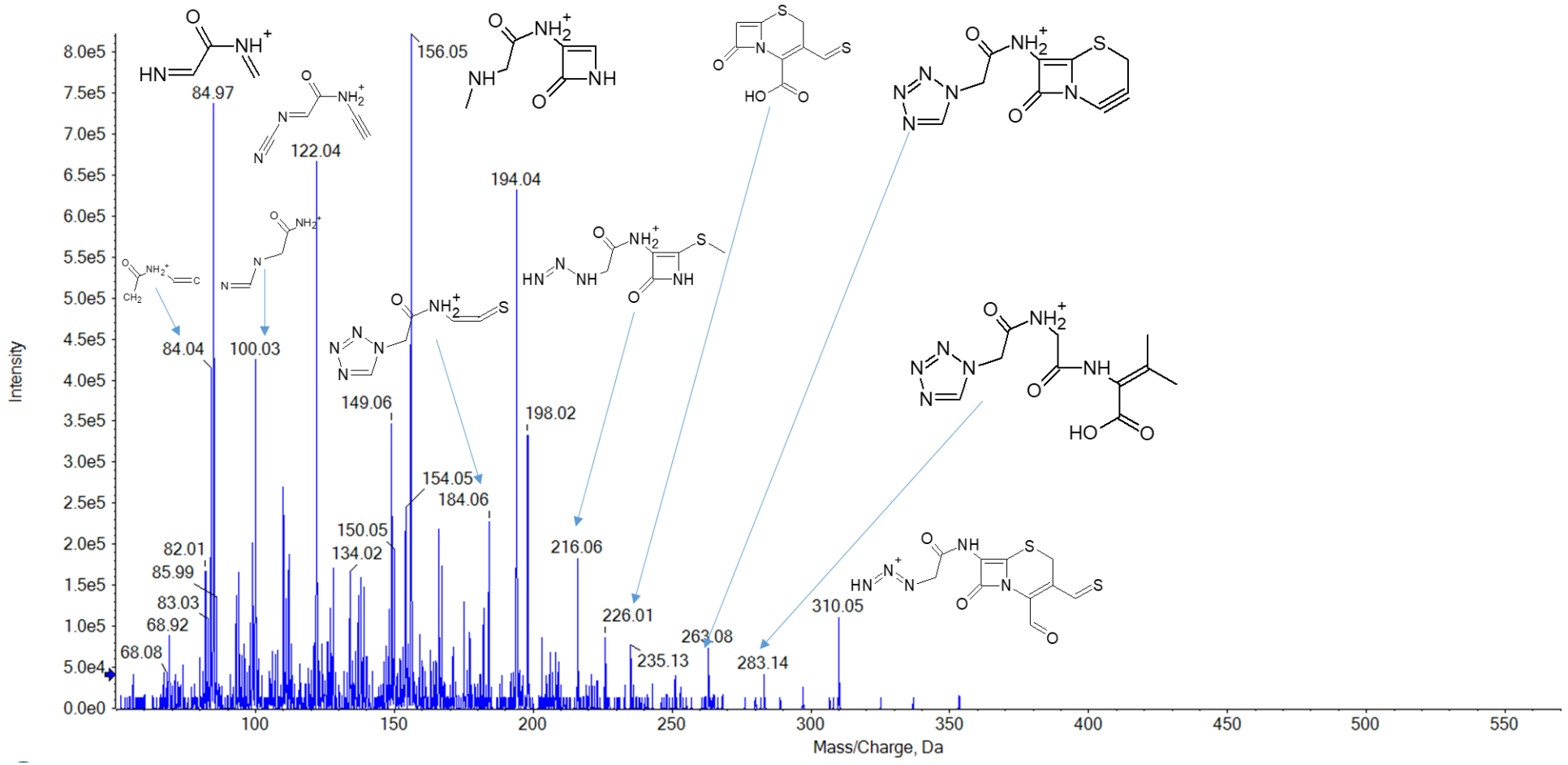

Figure S30. ESI (PI) MS/MS spectrum of CFZ-P8b.

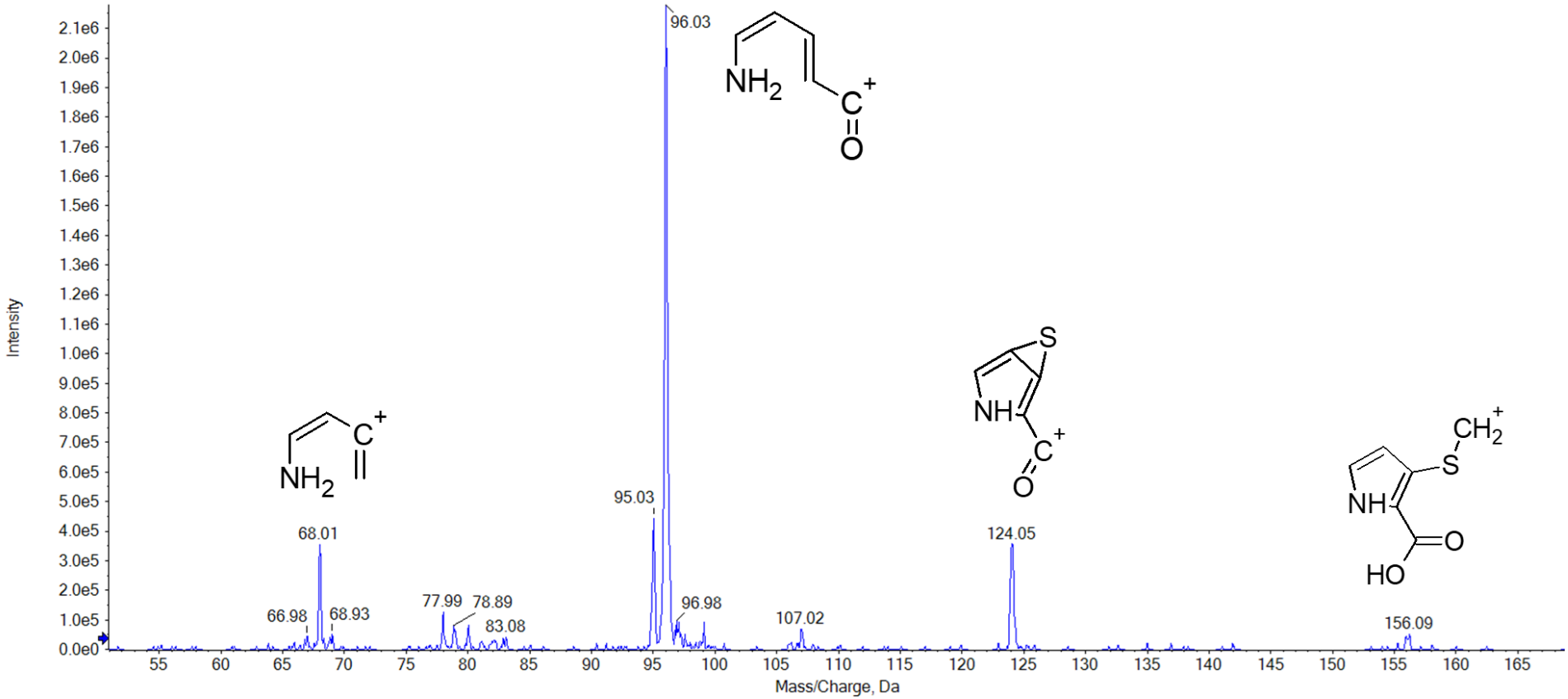

Figure S31. ESI (PI) MS/MS spectrum of IMI-P1.

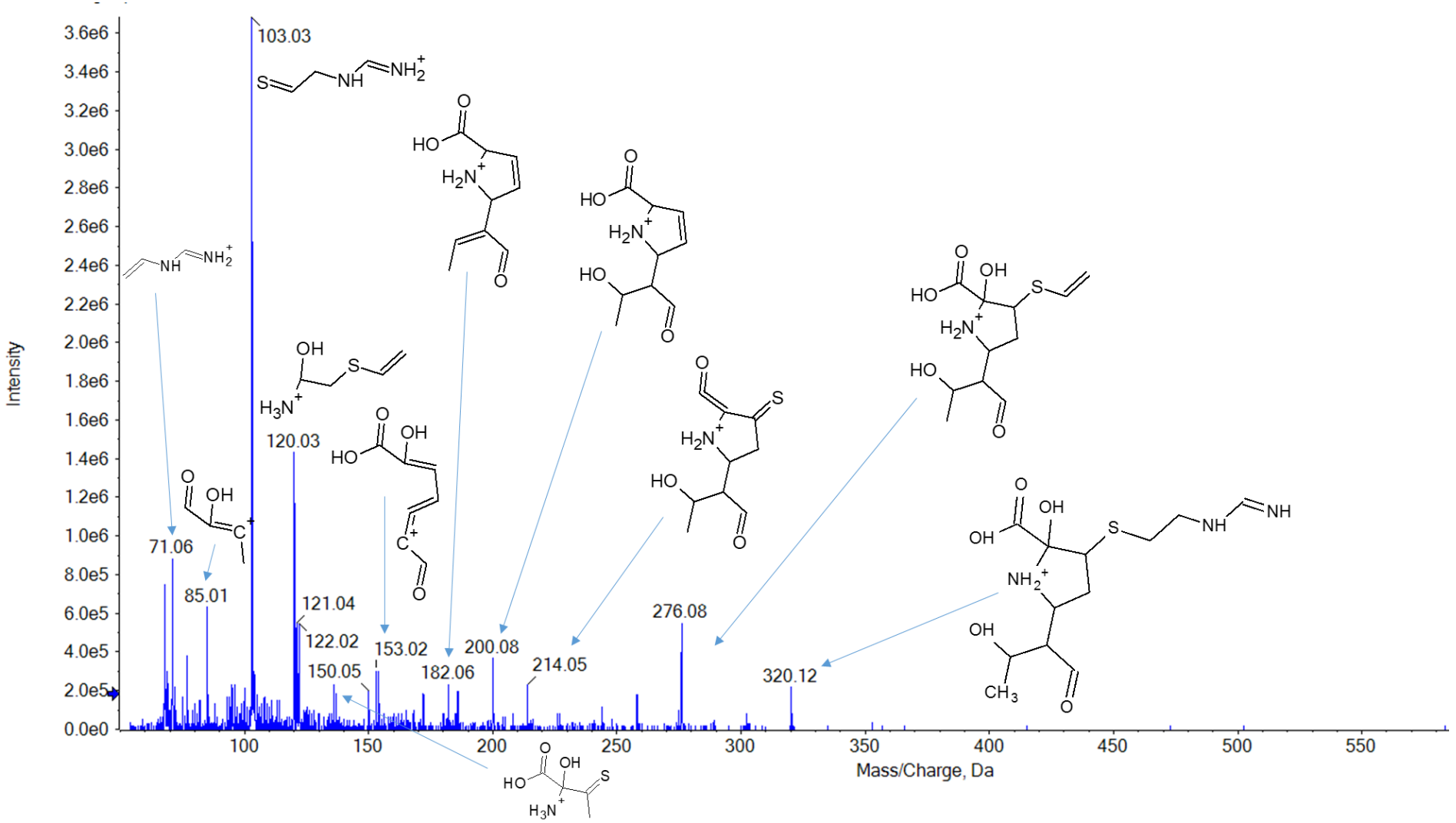

Figure S32. ESI (PI) MS/MS spectrum of IMI-P2.

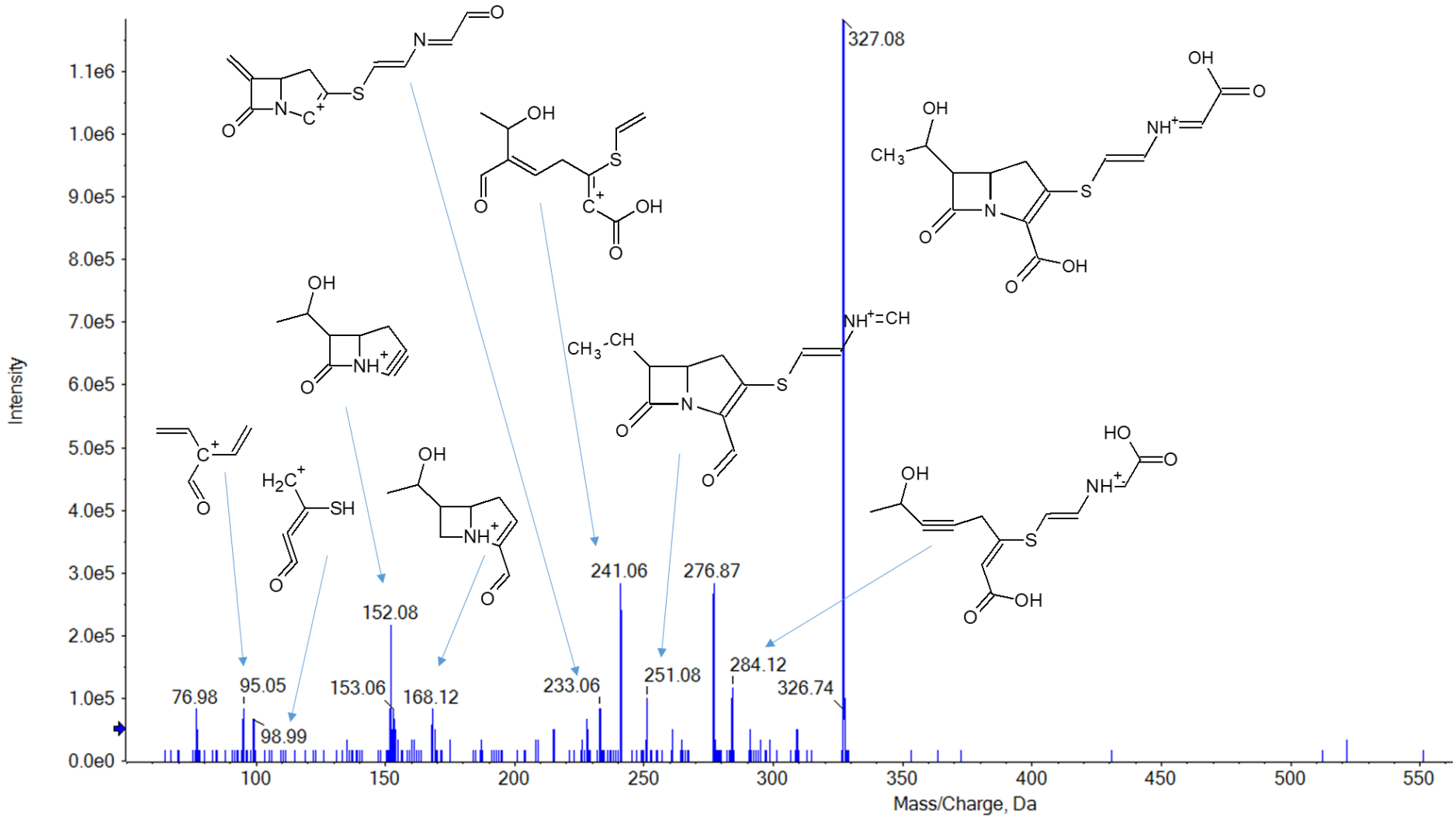

Figure S33. ESI (PI) MS/MS spectrum of IMI-P3.

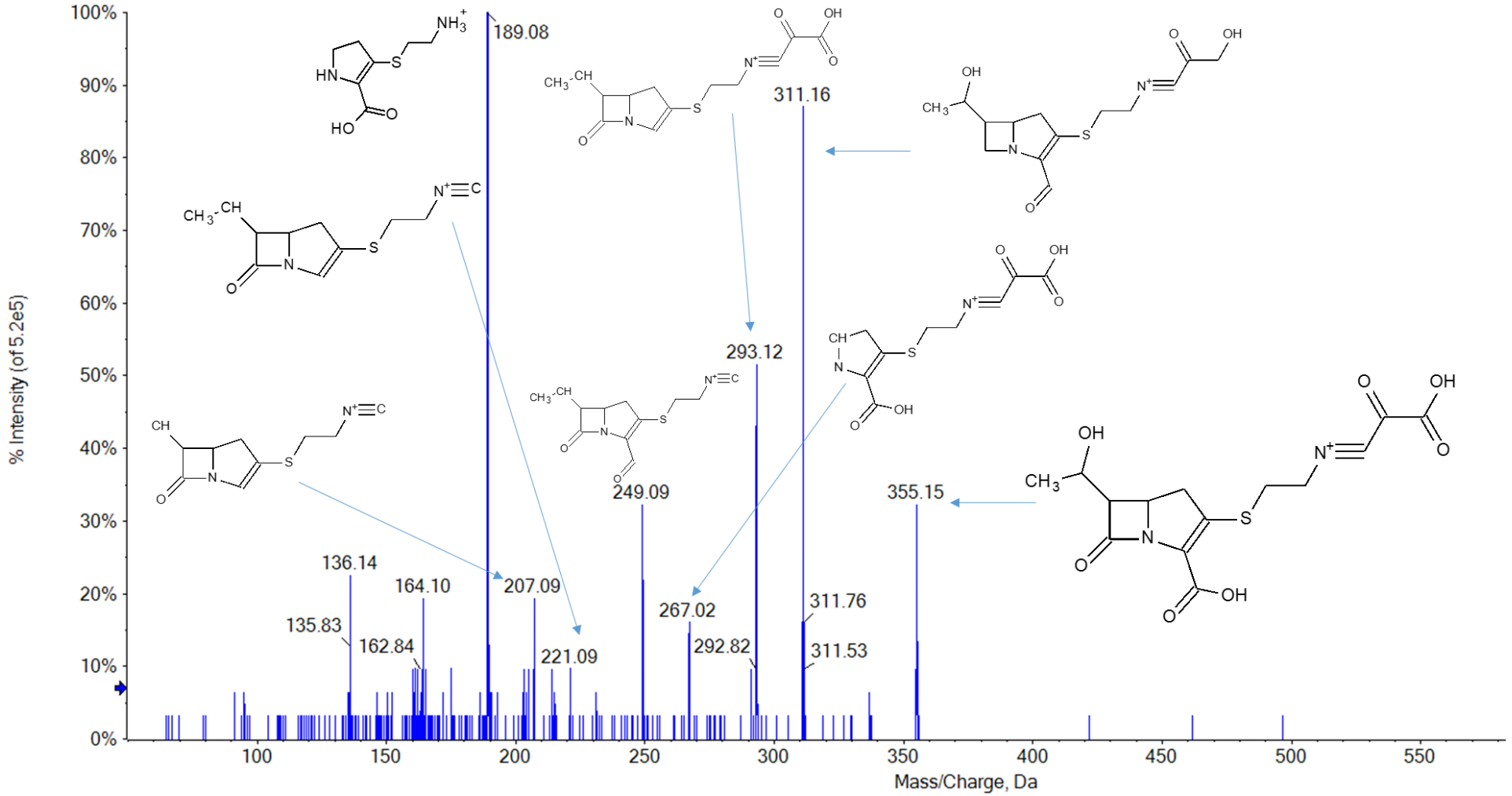

Figure S34. ESI (PI) MS/MS spectrum of IMI-P4.

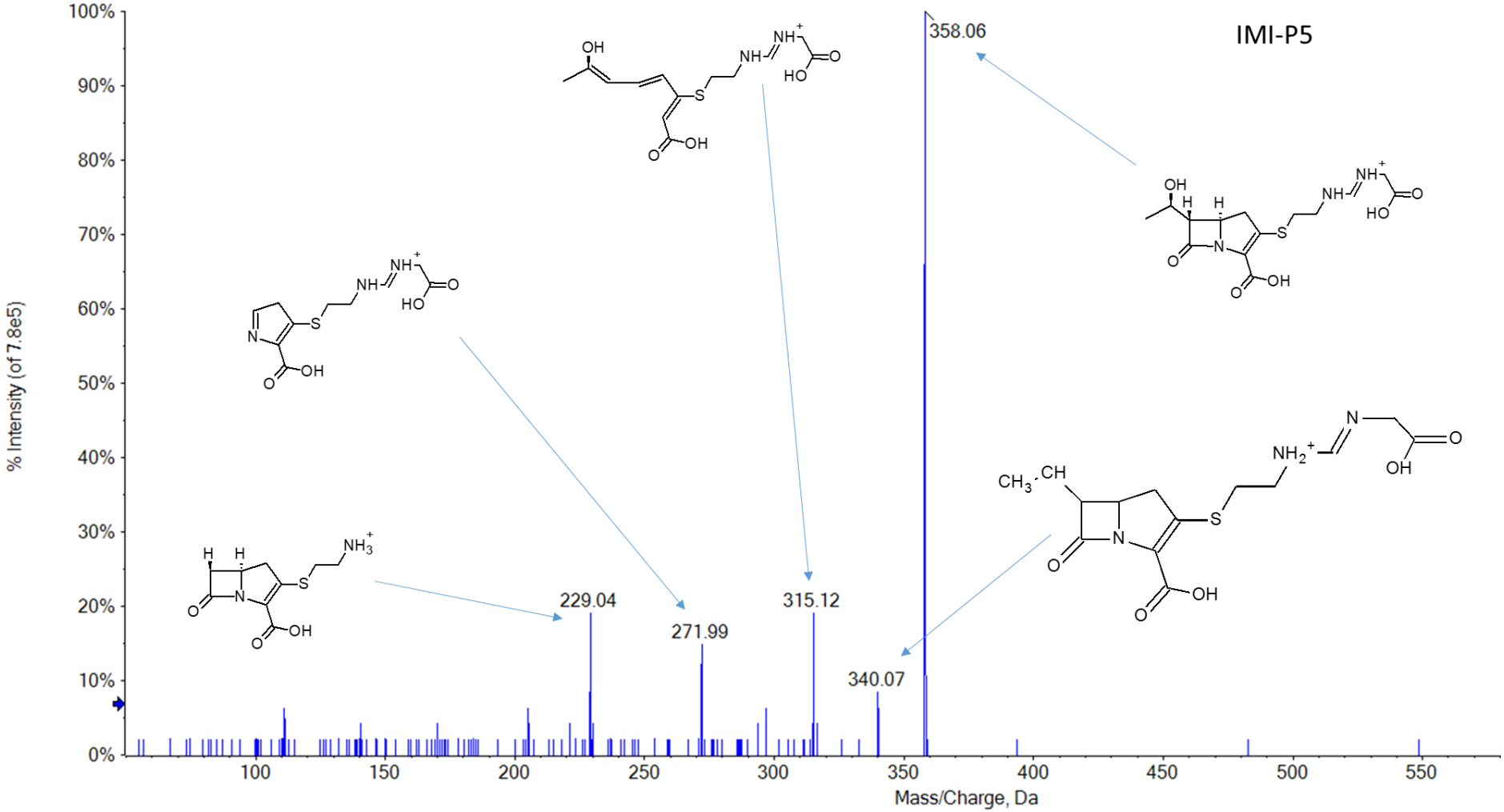

Figure S35. ESI (PI) MS/MS spectrum of IMI-P5.

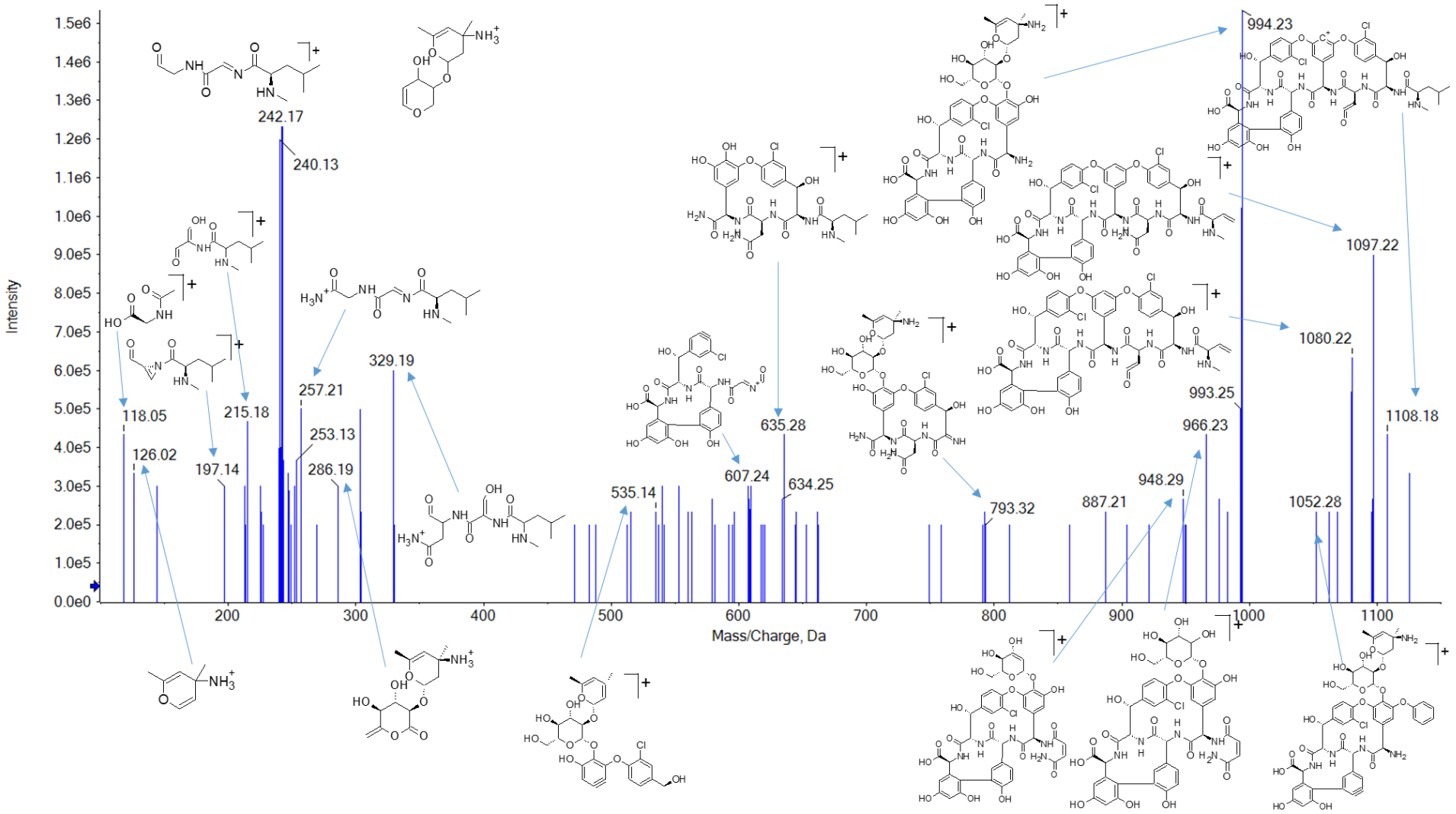

Figure S36. ESI (PI) MS/MS spectrum of VNM-P1.

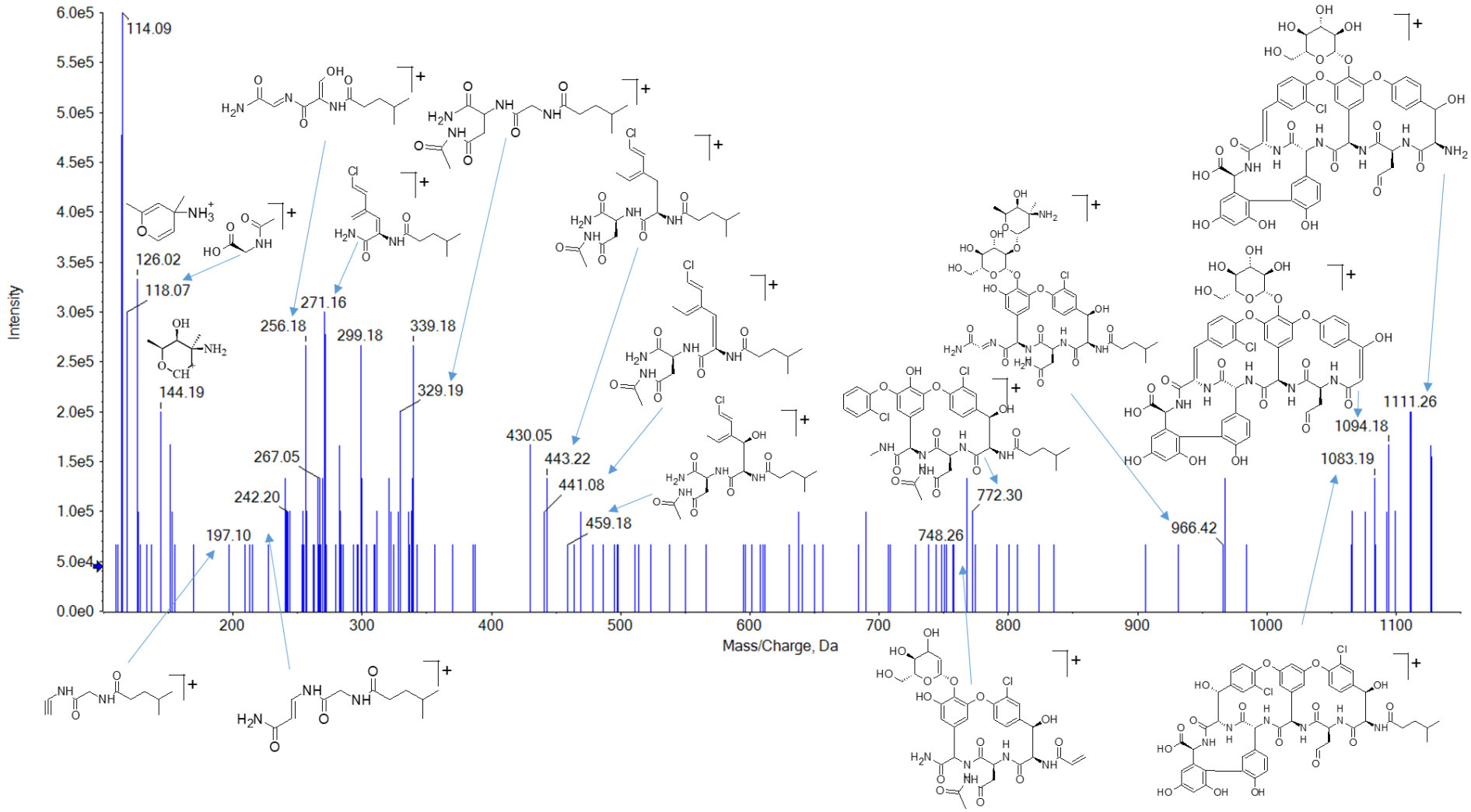

Figure S37. ESI (PI) MS/MS spectrum of VNM-P2.

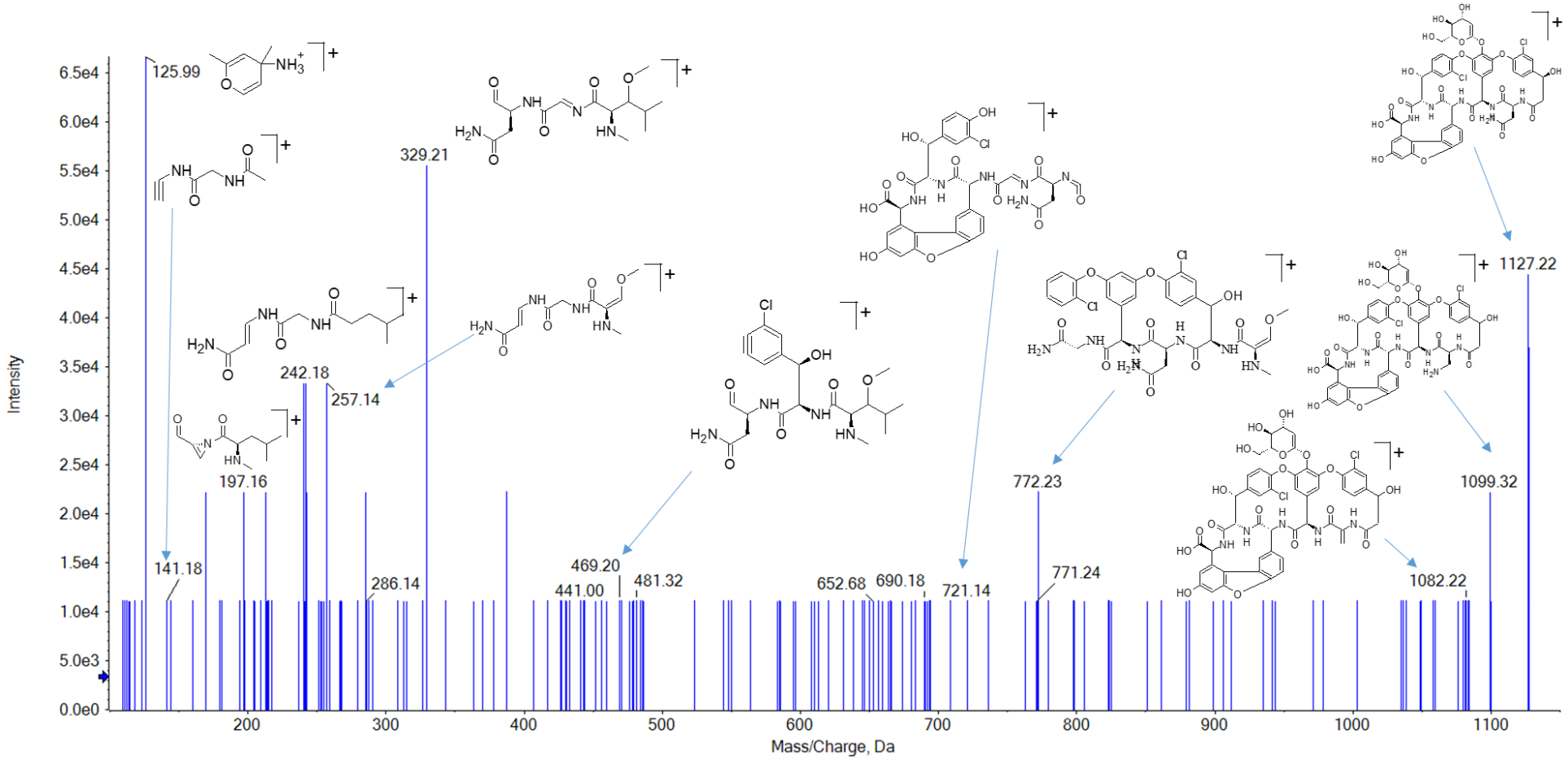

Figure S38. ESI (PI) MS/MS spectrum of VNM-P3.

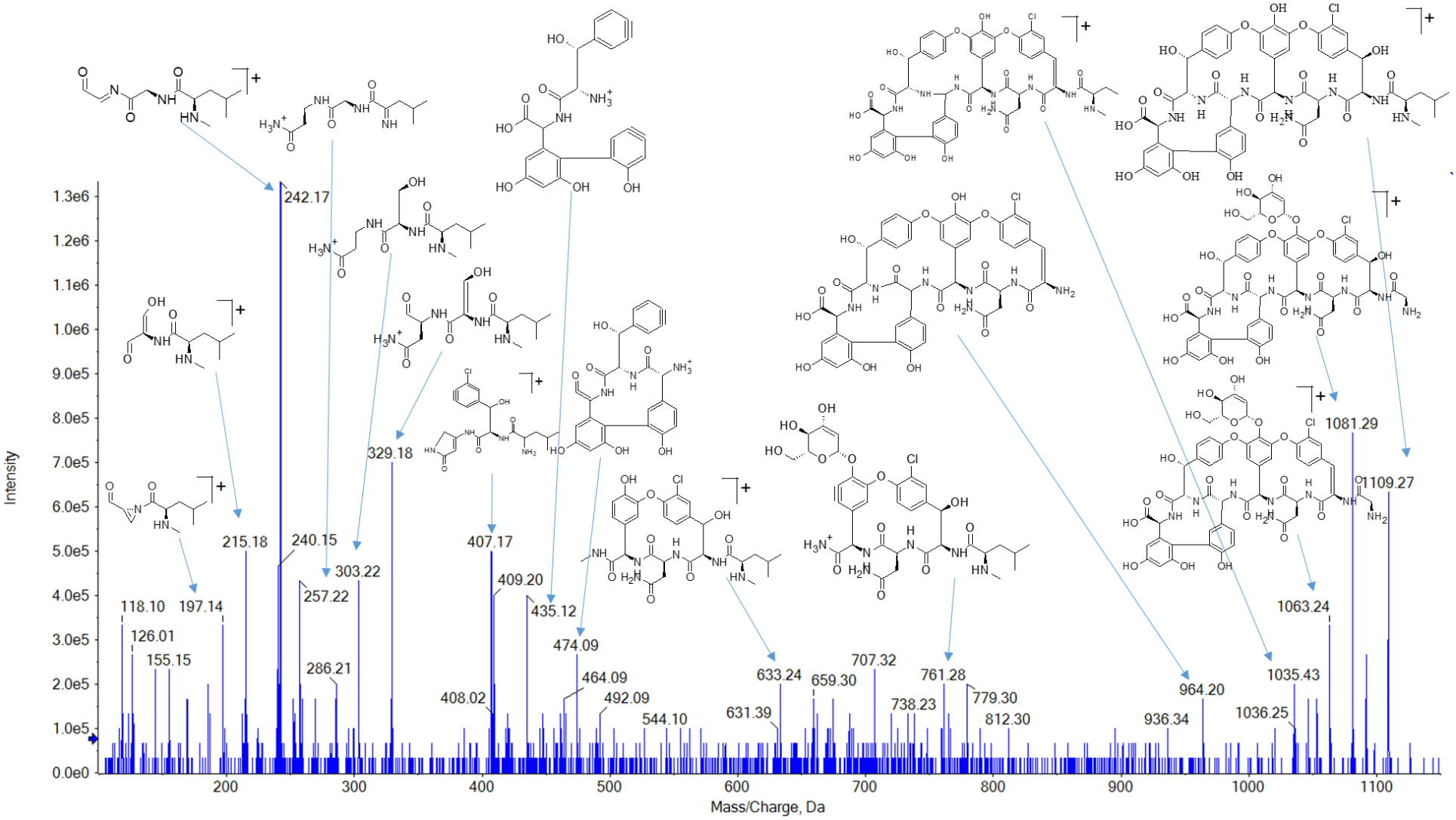

Figure S39. ESI (PI) MS/MS spectrum of VNM-P4a.

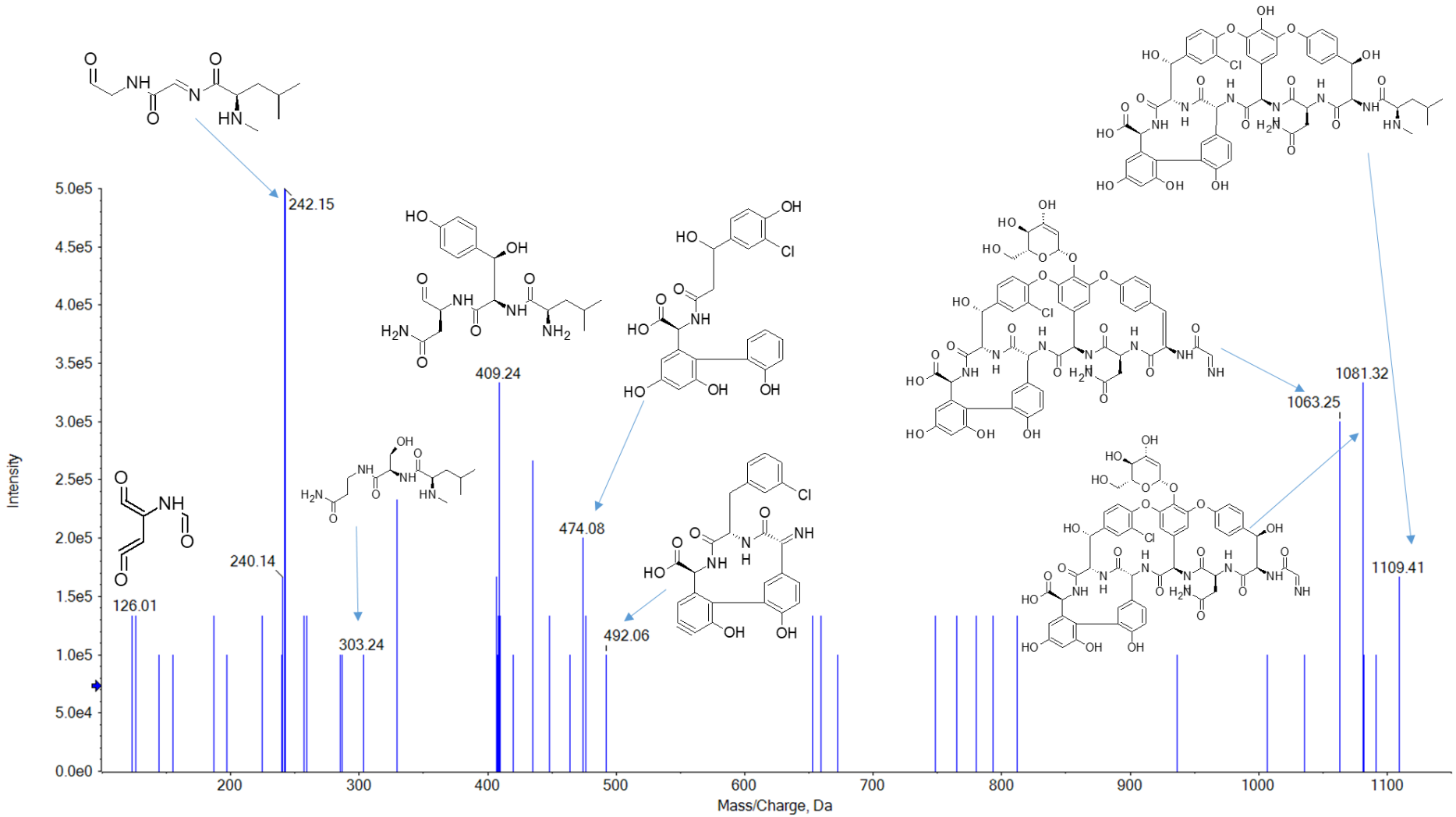

Figure S40. ESI (PI) MS/MS spectrum of VNM-P4b.

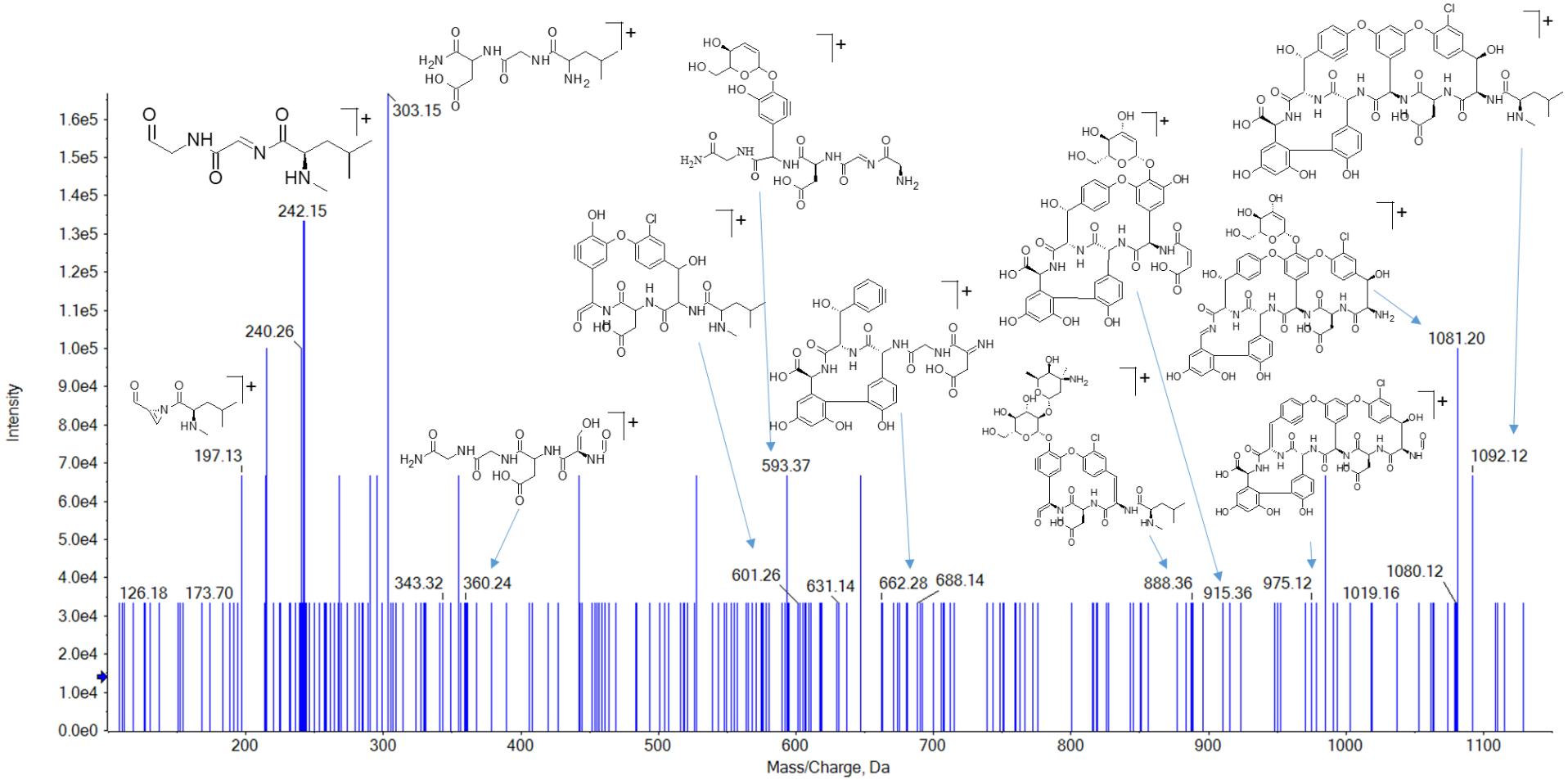

Figure S41. ESI (PI) MS/MS spectrum of VNM-P5a.

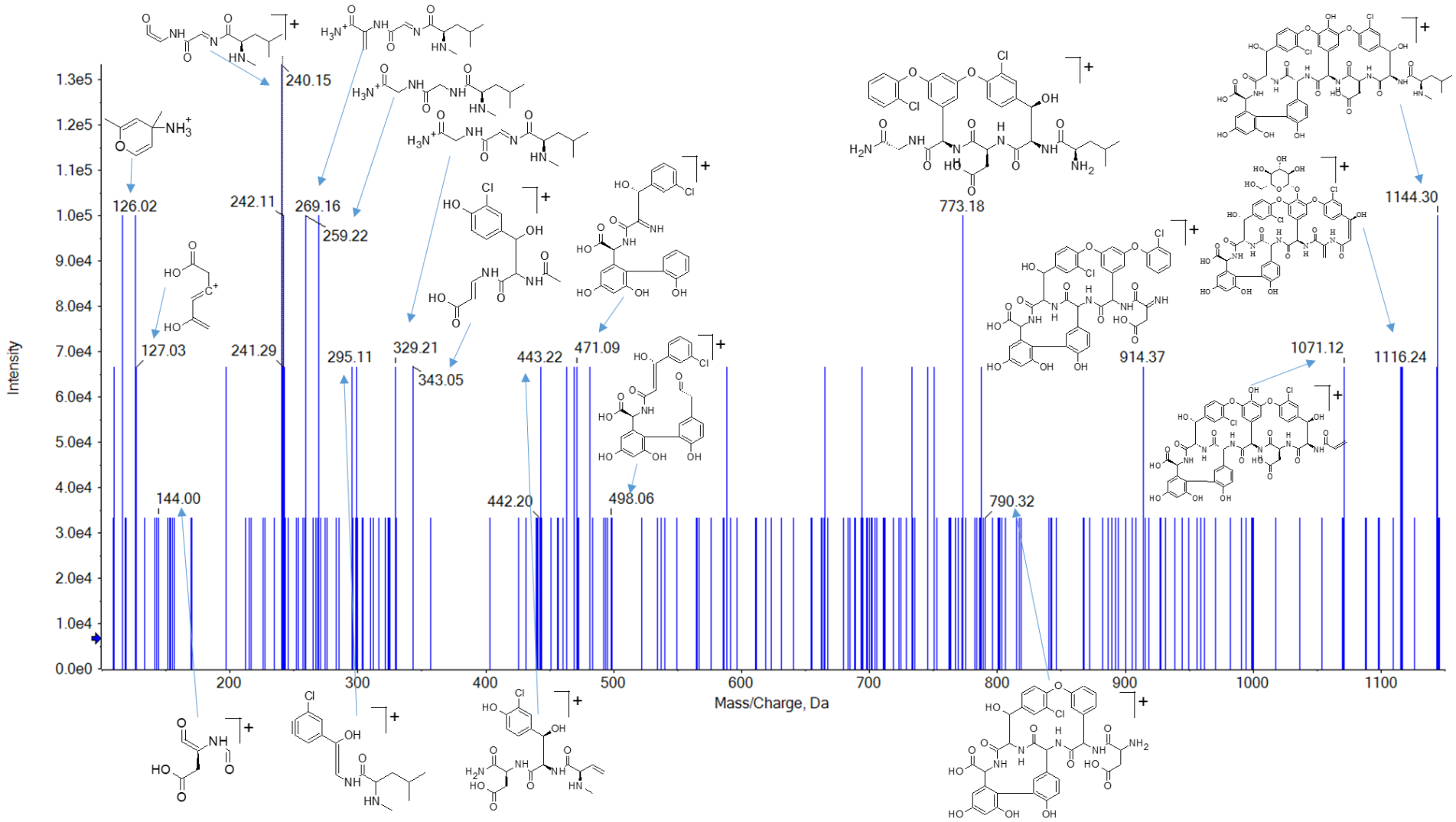

Figure S42. ESI (PI) MS/MS spectrum of VNM-P6a.

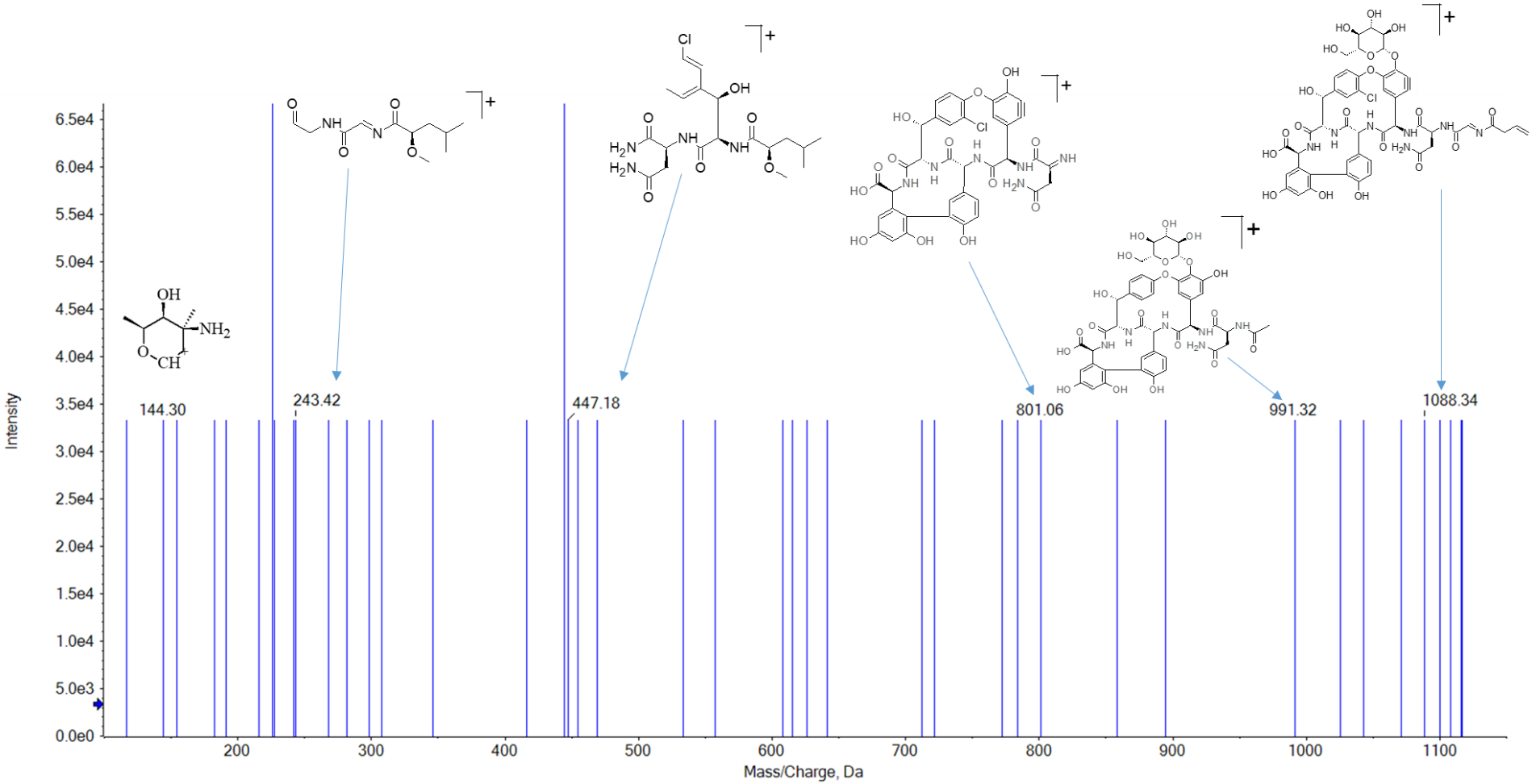

Figure S43. ESI (PI) MS/MS spectrum of VNM-P6b.

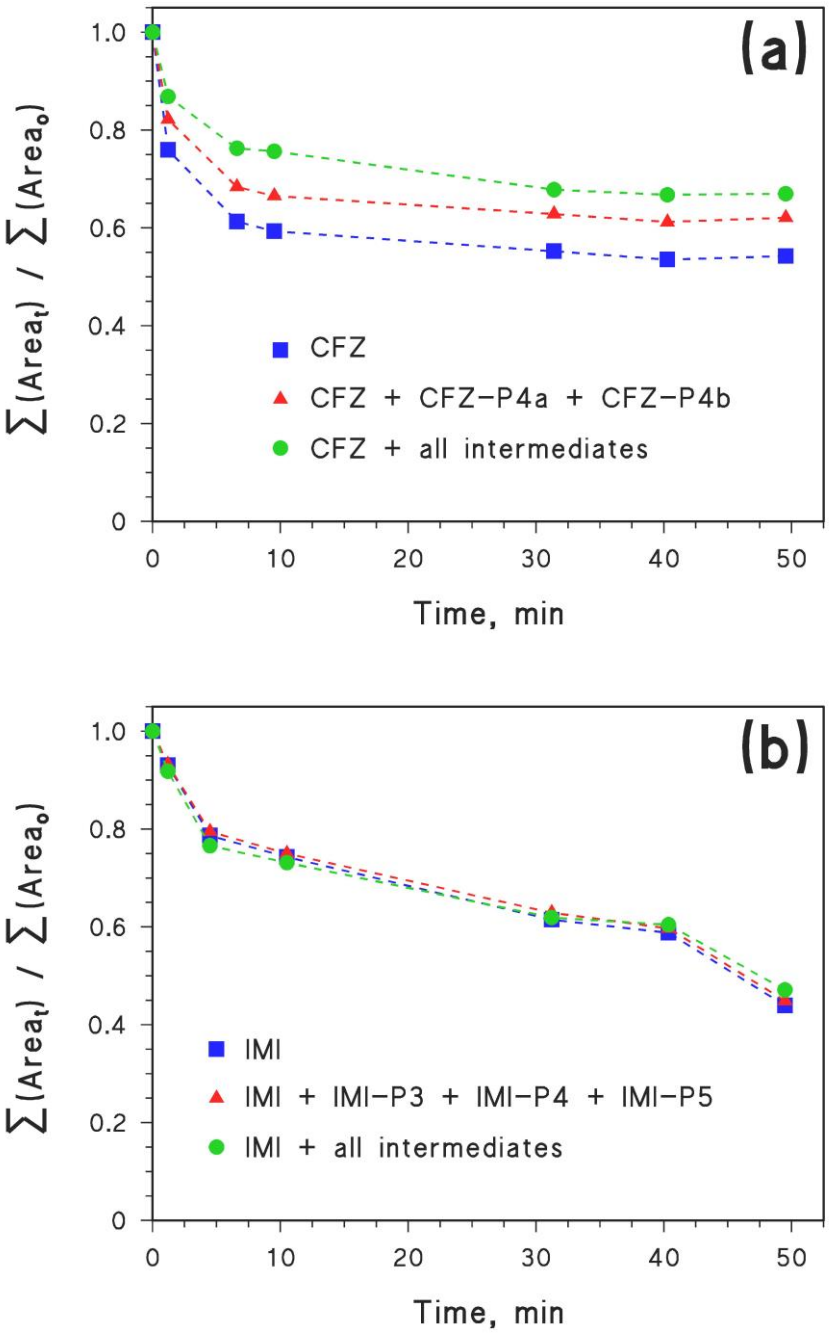

Figure S44. Time trends of the normalized peak areas of: *(i)* initial antibiotic; *(ii)* antibiotic plus the detected intermediates that retain an intact β-lactam ring; *(iii)* antibiotic plus all the detected intermediates. **(a)** cefazolin (CFZ); **(b)** imipenem (IMI).

Fenton conditions: 3×10^{-4} mol L^{-1} antibiotic, 3×10^{-4} mol L^{-1} H_2O_2 added twice (at 0 min and at 30 min), 0.03 g L^{-1} ZVI, pH 5 by H_2SO_4.